

An in-house code for studying the response of soil deposits in Mumbai city using 2-D equivalent linear and 1-D nonlinear approach

Raj Banerjee, Srijit Bandyopadhyay, Tarvinder Singh, Aniruddha Sengupta, G.R. Reddy, Justin Coleman & Chandrakanth Bolisetti

To cite this article: Raj Banerjee, Srijit Bandyopadhyay, Tarvinder Singh, Aniruddha Sengupta, G.R. Reddy, Justin Coleman & Chandrakanth Bolisetti (2020): An in-house code for studying the response of soil deposits in Mumbai city using 2-D equivalent linear and 1-D nonlinear approach, Geomechanics and Geoengineering

To link to this article: <https://doi.org/10.1080/17486025.2020.1728395>



Published online: 27 Feb 2020.



Submit your article to this journal [↗](#)



View related articles [↗](#)



View Crossmark data [↗](#)



An in-house code for studying the response of soil deposits in Mumbai city using 2-D equivalent linear and 1-D nonlinear approach

Raj Banerjee ^a, Srijit Bandyopadhyay^a, Tarvinder Singh^a, Aniruddha Sengupta^b, G.R. Reddy^a, Justin Coleman^c and Chandrakanth Bolisetti^c

^aScientist, Bhabha Atomic Research Center, Mumbai, India; ^bCivil Engineering Department, Indian Institute of Technology, Kharagpur, India; ^cIdaho National Laboratory, Seismic Research Group, Falls, ID, USA

ABSTRACT

For simulating any type of dynamic soil–structure interaction, a site response analysis is a necessary precursor. A 2-D equivalent linear model and a nonlinear model using hyperbolic tangent formulation are developed in-house for the purpose. Both the numerical models are validated by the experimental results on cohesionless soil conducted within a large-scale laminar box at Buffalo State University, New York and an open-source code DEEPSOIL. The non-linear soil behaviour of the laminar box is modelled by obtaining the normalised stiffness and damping ratio from torsional resonant column test. The validated program is used for prediction of the response behaviour at two sites in Mumbai. The ground response by equivalent linear and nonlinear method shows amplification factors of 2.95 for Site-1 and 3.55 for Site-2, 2.88 for Site-1 and 2.84 for Site-2, respectively. It is observed that the effects of the loading-unloading rules as well as the selection of the small strain damping values have a significant influence on the high-frequency content of the site-specific spectrum. The generated spectrum obtained from the nonlinear analysis may be used for any dynamic analysis at these locations with due regards to the values of small strain damping which is recommended to be around 1.0–1.5% for these sites.

ARTICLE HISTORY

Received 30 November 2019
Accepted 7 February 2020

KEYWORDS

Response spectrum;
equivalent linear analysis;
non-linear analysis; laminar
box test

1. Introduction

The area considered in this study is in the city of Mumbai, the commercial capital of India. The city of Mumbai has its centre at 19.0760° N, 72.8777° E and spreading over an area of 603.4 km². The city has a population of approximately 20.7 million. Mumbai is in Seismic Zone III as per the Indian Building code (IS:1893(Part 1) 2002), signifying that the city may be subjected to an intensity of VII damage as per MSK64 intensity scale (a region with moderate seismic hazard). The Mumbai region has experienced low to moderate level of seismic activity (Jaiswal and Sinha 2007). Some of the large and damaging earthquakes affecting the region are Koyna (1967), Killari (1993), Jabalpur (1997) and Kachchh (2001) Earthquakes. Mumbai is located near the Panvel seismic source zone, which is known to be seismically active (Dessai and Bertrand 1995, Nandy 1995). Therefore, seismic ground response analysis is required to develop the site-specific response spectrum for the design of important superstructures in the region. The one-dimensional ground response analysis is a commonly used method to estimate the ground responses under earthquake excitation in both equivalent linear and non-linear domains. The idea behind performing the exercise in both the domains

is to study the conditions under which the two methods produce consistent and divergent estimates of site amplification. Stewart *et al.* (2008) have compared the results of equivalent linear and non-linear analyses performed by Silva *et al.* (2000) and noted that there is a good agreement between the two approaches over most of the frequency range from 0.1 to 100 Hz for stiff soils subject to motions with PGA less than 0.4 g. However, at larger shaking levels (PGA ≥ 0.4 g), non-linear responses are larger than the equivalent linear responses for frequencies higher than 10 Hz. Kramer and Paulsen (2004) have conducted an informal survey that has shown that the equivalent linear analyses provide reasonable results for shear strains less than 1% to 2%. Kaklamanos *et al.* (2013) have evaluated the accuracy and the precision of linear and equivalent linear site response analyses using 100 KiK-net downhole arrays in Japan. They have found that a non-linear analysis is preferred over an equivalent linear analysis for maximum shear strains greater than 0.05%. Zalachoris and Rathje (2015) have evaluated equivalent linear and non-linear site response analyses using 9 borehole arrays in Japan, La Cienega and Lotung. They also have identified similar thresholds to those proposed by Kaklamanos *et al.* (2013).

In this study, 2-D plane strain site response analyses have been performed for two sites (Site-1 and Site-2) near Mumbai by equivalent linear method for different levels of ground shaking (that is, for different frequency content, duration, etc.). An in-house code with lumped mass model (element mass matrix) and pure shear boundary conditions, performing time-domain integration of the equations of motion step-by-step, has been developed for this purpose. It assumes that the soil layers are horizontal and the response of a soil site is predominantly due to the horizontally-polarised shear waves that propagate vertically from the underlying bedrock. An iterative procedure is used to obtain the values of the shear modulus (G) and the damping ratio (D) compatible with the representative effective shear strain in each soil layer. Though the equivalent linear method is fast and provides reasonable estimates for most of the practical problems, it is an approximate solution to the actual non-linear seismic ground response. Hence, to compare the equivalent linear results, the actual non-linear response has been analysed by developing a 1-D total stress nonlinear model in time domain, for studying the behaviour of the sites located in Mumbai. The method of analysis employed in time-stepping procedures can in some respects be compared to the analysis of a structural response to input ground motion (Clough and Penzien 1993, Chopra 2001). The system is represented by a series of lumped masses or discretised into elements with appropriate boundary conditions. The system of coupled equations is discretised temporally and a time-stepping scheme, Newmark's β -method (Newmark 1959) is employed to solve the system of equations and to obtain the response at each time step. In addition, Masing rules (Masing 1926) and extended Masing rules (Pyke 1979, Vucetic 1990) are used in conjunction with the backbone curves to describe the unloading-reloading behaviour of a soil. Special emphasis has been given on the effect of the small strain damping value and the loading-unloading rules on the high-frequency content of the response spectrum as it is an area of interest for the calculation of seismic demands for nuclear (or stiff) facilities. The small strain damping simulates damping ratio at small strains ($\epsilon < 0.0001\%$ to 0.01%). It is needed because the hyperbolic model used in the nonlinear analyses underestimates damping ratio (as hyperbolic model is linear at small strains) when compared with the experimental results. The value of the damping ratio to be taken is a grey area which has been addressed in this study and it has been found that the value of the small strain damping is a site dependant property which is found to vary between 1.0% and 1.5% for these sites but sometimes it may be even higher than the predicted range to remove

the high-frequency noises. In similar lines, not much effect on the spectral values has been found due to the change in the unloading-reloading behaviour of a soil as there is no generation of artificial frequencies (or noise) due to the change in these rules; hence, it is a parameter which requires less attention.

2. Methods of analysis and model validation

A program has been developed for studying the ground responses at two typical Mumbai soil sites by performing 2-D equivalent linear analyses in time domain and using pure shear (Multi-point constraint (Abel and Shephard 1979) boundary condition. This type of boundary condition is used to simulate pure shear type of movement in a soil column in which the unwanted reflections from the boundaries are minimised to a significant extent in comparison to the absorbing boundaries. Further, a 1-D total stress nonlinear analysis of multiple degree of freedom lumped mass, spring and dashpot systems with appropriate boundary conditions has also been developed to compare the results obtained from the equivalent linear analysis.

In the equivalent linear analysis, an iterative approach is followed (Kramer 2005), in which, the initial estimates of the values of the shear modulus, G_i and damping ratio, D_i , corresponding to small strains, are assumed for each soil layer. The estimated G_i and D_i are used to compute the ground response, including the time histories of shear strain for each layer. The effective shear strain in each layer is determined from the maximum shear strain in the computed shear strain time history. From this effective shear strain, new values for G_{i+1} and D_{i+1} are estimated for the next iteration. The above steps are repeated until the difference between the previous and the new values is less than 5–10%. The iteration converges within 3 to 4 steps, normally (Schnabel *et al.* 1972). In the equivalent linear approach, the following dynamic equation of equilibrium is solved in discrete time increments using time domain analysis.

$$[M]\{\ddot{u}(t)\} + [C]\{\dot{u}(t)\} + [K]\{u(t)\} = [M][I]\{\ddot{u}_g(t)\} \quad (1)$$

where $[M]$ is the lumped mass matrix, $[K]$ is the stiffness matrix, $[I]$ is the influence matrix (equal to 1 in the direction of the application of motion, and 0 in the direction, where no motion is applied) and $[C]$ is the damping matrix of the soil. The above equation is solved numerically at each time step using the constant average acceleration method (Newmark 1959). The base of the soil column is modelled as infinitely stiff. For the i^{th} layer of the soil, the soil mass is lumped at each node of an 8-noded,

2-D quadrilateral element ($= \rho V/8$, where ρ is the density of soil, V is the volume of the element). The formulation of the stiffness matrix requires the following basic definition:

$$[K] = \iint [B]^T [D] [B] dv \quad (2)$$

which in isoparametric formulation is expressed as:

$$[K] = t \iint_{-1}^1 [B]^T [D] [B] |J| d\xi d\eta \quad (3)$$

where $\eta = y/a$, $\xi = x/a$ where 'a' is the half of the element size. 't' is the out of plane thickness of the element. [D] is the constitutive matrix in plane strain and given by:

$$[D] = \frac{E}{(1 + \nu)(1 - 2\nu)} \begin{bmatrix} 1 - \nu & \nu & 0 \\ \nu & 1 - \nu & 0 \\ 0 & 0 & \frac{1-2\nu}{2} \end{bmatrix} \quad (4)$$

in which, E is the elastic modulus and ν is the Poisson's ratio. For the formulation of the B-matrix, the following shape functions for an 8-noded element are defined:

$$\begin{aligned} N_1 &= \frac{1}{4}(1 - \xi)(1 - \eta)(-\xi - \eta - 1) \\ N_2 &= \frac{1}{4}(1 + \xi)(1 - \eta)(\xi - \eta - 1) \\ N_3 &= \frac{1}{4}(1 + \xi)(1 + \eta)(\xi + \eta - 1) \\ N_4 &= \frac{1}{4}(1 - \xi)(1 + \eta)(-\xi + \eta - 1) \\ N_5 &= \frac{1}{2}(1 - \xi)(1 - \eta)(1 + \xi) \\ N_6 &= \frac{1}{2}(1 + \xi)(1 - \eta)(1 + \eta) \\ N_7 &= \frac{1}{2}(1 - \xi)(1 + \eta)(1 + \xi) \\ N_8 &= \frac{1}{2}(1 - \xi)(1 - \eta)(1 + \eta) \end{aligned} \quad (5)$$

The node numbering in a single element is shown in Figure 1. The [C] matrix is a combination of elemental mass and stiffness matrices and is of the form (Rayleigh and Lindsay 1945)

$$[C] = \alpha_R [M] + \beta_R [K] \quad (6)$$

The values of α_R and β_R are calculated by considering the first and the third natural frequencies of a soil column. In the equivalent linear analysis, the damping ratio is calculated with the variation of shear strain for a soil. For a frequency-independent damping ratio, the formulation of damping for a multi-layered soil is followed as per (Hashash and Park 2002). The soil column is modelled using 2-D, plane strain, 8-noded, quadratic, quadrilateral element with two degrees of freedom (horizontal and vertical displacements) at each node. A rigid

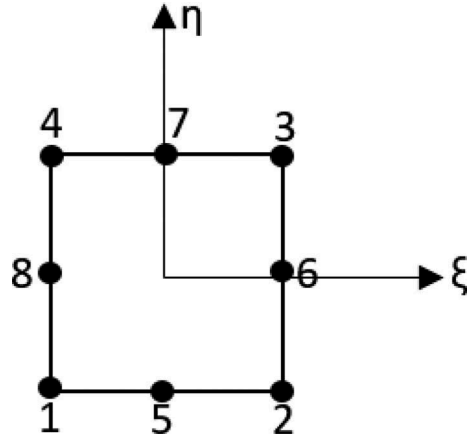


Figure 1. Node numbering in an 8-noded quadratic quadrilateral element.

element is utilised to impose a multi-point constraint. A rigid element is a 1-D truss element with high axial stiffness ($AE/L = w$) and two degree of freedom at each node. It is connected to the two nodes of the lateral boundaries of the soil column. The axial stiffness is made high so that there is negligible axial strain in the bar element which implies that the deflection of the end nodes is same. One node acts as the 'master' and another node acts as a 'slave'. The constraint equation that ties the horizontal and vertical degree of freedom is written in the following form (Cook *et al.* 1989),

$$[B][u] = [A] \quad (7)$$

where B and A are constants. For homogeneous constraints, the value of [A] is equal to zero. The equation may be written in a modified form as,

$$[Q] = [B][u] - [A] \quad (8)$$

$[Q] = 0$ implies the satisfaction of the constraints. 'Penalty augmentation' (Cook *et al.* 1989) is used for implementation of the constraints at the boundary degrees of freedom. Each multi-point constraint is viewed as the presence of a fictitious elastic structural element called penalty element (w) that enforces it approximately. This element is parametrised by a numerical weight. The multi-point constraints are imposed by modifying the assembled stiffness matrix which is submitted to the equation solver as,

$$[K_{modified}] = [K] + [B]^T w [B] \quad (9)$$

If $w = 0$, then the constraints are ignored, hence the selection of the appropriate weights are necessary to minimise ill-conditioned solution (with respect to inversion of the stiffness matrix) as well as to avoid mesh locking. For instance, if we choose the horizontal nodal displacements at nodes 4 and 8, $u_{4x} = u_{8x}$, then it

may be written as $u_{4x}-u_{8x} = 0$, which is a homogeneous constraint. It may be written in the matrix form as,

$$[1 \ -1] \begin{bmatrix} u_{4x} \\ u_{8x} \end{bmatrix} = 0 \quad (10)$$

where $[B] = [1 \ -1]$ and $[B]^T w [B] = w \begin{bmatrix} 1 & -1 \\ -1 & 1 \end{bmatrix}$

The above matrix is incorporated into the assembled stiffness matrix at the appropriate locations of the degree of freedom. It generally implies the addition of an axially rigid truss element with axial stiffness (w) to the two tied nodes. The trade-off value of weights is difficult to find, which will encompass all the problems. A rule is followed in which the weights are chosen typically on the order of 10^6 to 10^7 for double precision (64-bit processor) to avoid numerical difficulty (Cook *et al.* 1989). At the bottom of the model, 'rigid' base is assumed and the formulation is done in terms of total displacements. It may be noted that this traditional approach assumes that the total motion at the foundation base is known in terms of acceleration and the boundary degrees of freedom for the relative displacements are constrained to zero (Zienkiewicz *et al.* 1990).

The present nonlinear model is based on total stress analysis of multiple degree of freedom lumped mass systems with appropriate boundary conditions. The system of coupled equations, as shown in Equation (1), is discretised temporally and a time-stepping scheme such as the 'Newmark Average Acceleration' method (Newmark 1959) is employed to solve the system of equations and to obtain the response at each time step. The formulation of stiffness and damping matrix for lumped mass systems is the same as the one given in DEEPSOIL (Hashash and Park 2002, Hashash *et al.* 2012). In this formulation for the viscous damping matrix, the value of stiffness matrix $[K]$ is not updated at each time step which implies that the viscous damping matrix is not updated at each time step. To capture the hysteretic damping in the system, the rules of loading-unloading cycles are followed as proposed by Masing (1926) and Xiaojun and Zheneng (1993). As the extended Masing rules (Pyke 1979, Vucetic 1990) cannot be converted into simple functional form, hence in this model, a modified dynamic stress-strain relationship is used which simplifies the modelling of the extended Masing rules. As extended Masing rules cannot be converted to simple functional form, hence this study uses the equations given by Xiaojun and Zheneng (1993), which has a complete functional form for loading, unloading and reloading. The corresponding equations are detailed in Xiaojun and Zheneng (1993). The stiffness matrix $[K]$ is assembled at each time step using

the incremental properties of soil layers obtained from a constitutive model that describes the cyclic stress-strain characteristics (backbone curves) of the soil layer. The modulus reduction curves, whereby the dynamic modulus of soil decreases with strain, is used to define the backbone curves. In this model, the equation of backbone curve is given by Equation (11),

$$\tau = \frac{\gamma}{A + B\gamma} \quad (11)$$

where τ is the shear stress, γ is the shear strain, γ_{ref} is the reference shear strain, $A = 1/G_{max}$ and $B = 1/\gamma_{ref}/G_{max}$. The value of γ_{ref} is used to adjust the shape of the backbone curve to get a proper match with the modulus reduction curve of a soil.

The base of the soil column is assumed to be infinitely stiff. Each individual soil layer is assumed to have a nonlinear spring (which considers for hysteretic damping), and a dashpot for simulating small strain damping in soil (which is optional to use in this model). The lumping the mass at each node of the soil column based on the adjacent upper and lower soil properties are used for the formation of mass matrix. The formulation of stiffness matrix is such that it is updated at each time increment, and the stiffness k_i for i^{th} soil layer is given as $k_i = G_i/h_i = (\tau(\gamma_i) - \tau(\gamma_i - \gamma_{i-1})) / (h_i (\gamma_i - \gamma_{i-1}))$, which shows that the value of tangent modulus, G is used to update the stiffness matrix at each solution step. The time step for solving the nonlinear program is decided by the results obtained by choosing different time steps and the optimum time step is selected for the problem in which the results (in terms of acceleration, shear strain, etc.) does not differ by more than 1% from the previous one. Generally, a time step of 0.001 sec is accurate enough to predict the nonlinear response of a soil, and is used in this study.

Prior to the development of parameter selection and its usage for nonlinear analysis, it is important to verify the constitutive model implementation to ensure that the soil behaviour is modelled properly. Element testing is performed for this developed nonlinear model, which comprises of studying the response of a nonlinear single-degree-of-freedom system. Three types of analyses are performed corresponding to different loading patterns (symmetric, asymmetric and reversal loadings till failure). These analyses are performed by specifying a shear strain history and then calculating a shear stress history from the constitutive model.

The first type is a sinusoidal strain history with constant amplitude. The purpose of using such loading is to check if stress accumulates in one direction under symmetric loading, which may occur with some Masing-type

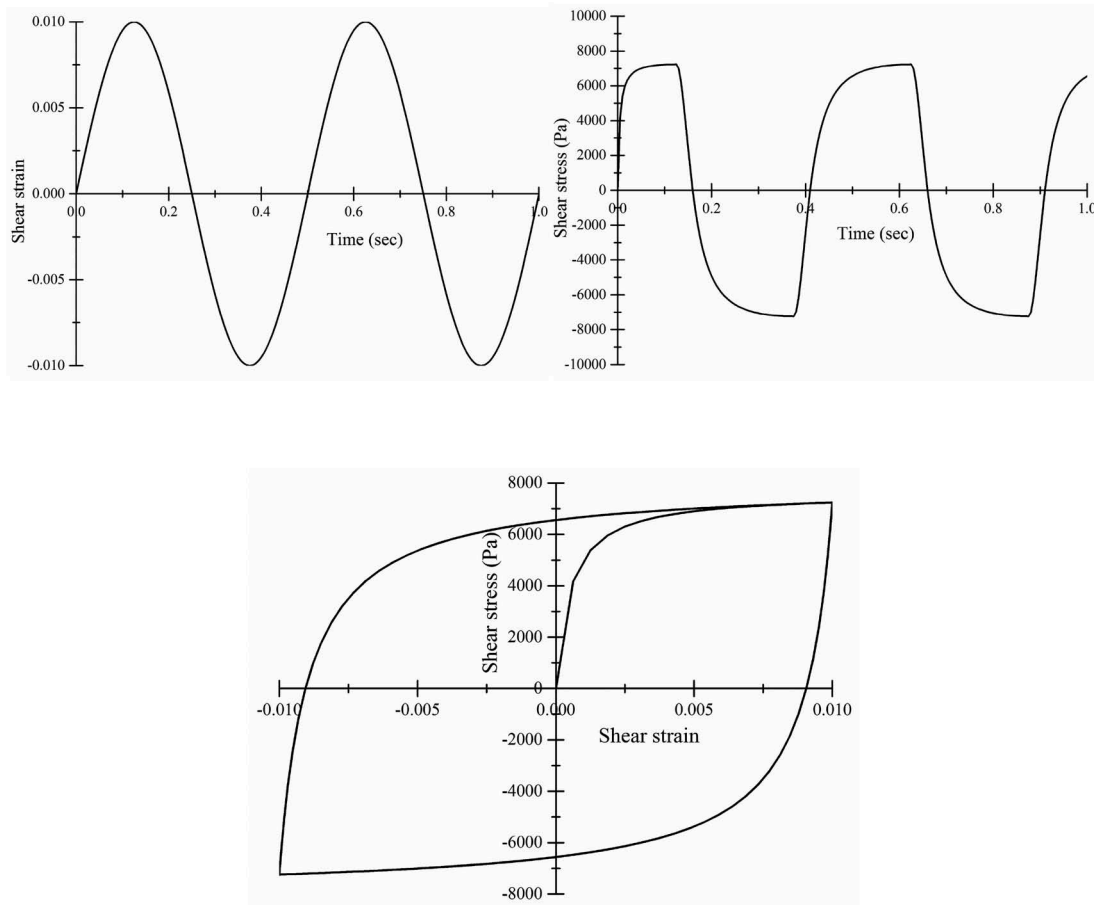


Figure 2. Behaviour of soil column with sinusoidal strain of constant amplitude.

unload/reload models. The predicted stress history from the nonlinear code is in-phase with the imposed strain history as shown in [Figure 2](#).

The second type of sinusoidal loading history gradually ramps the amplitude up to 1% and then gradually decreases back to zero. This is to test constitutive behaviour for successive cycles of different amplitude. As shown in [Figure 3](#), the predicted stress histories are all in-phase with the imposed strain history. Furthermore, the change in the stress amplitude follows the trend of strain amplitude. This gives us an idea that the developed model does satisfy the Masing and the extended Masing rules.

3. Validation by geotechnical laminar box tests

For the validation of the model in equivalent linear and nonlinear domains, the results of laboratory tests on F-55 Ottawa sand performed in a large-scale geotechnical laminar box (GLB) at the Buffalo State University, New York (Coleman *et al.* 2016) have been utilised. The GLB is composed of 40 laminate rings stacked on top of each other and separated by ball bearings. The laminates

are free to move laterally due to the frictionless bearings thereby allowing shear deformation of the soil contained within the box, which is numerically implemented by pure shear boundaries in this study. The box is lined with a custom 2.67 mm thick assembly of Firestone EPDM rubber. This rubber liner contains the soil material inside the GLB and prevents spillage of soil through the bearing-gaps between laminates. A uniaxial motion in the form of a sinusoidal wave or actual earthquake motion is applied at the bottom of the GLB by actuators. The motion applied to the GLB base propagates up through the soil column within the GLB to the free top of the box. The interior dimensions of the GLB are 4.97 m in E-W direction, 2.74 m in N-S direction and 6.09 m in height. Each laminate including space for the bearings is 0.1524 m in height. There are 40 such laminates in the box. The box is filled with the sand up to a depth of 5.2 m. The experimental setup of the geotechnical laminar box is shown in [Figure 4](#). The Ottawa F-55 sand is medium-grained sand with the mean particle size (D_{50}) equal to 0.258 mm and contains less than 1% fines. The sand grains are mainly rounded, colourless pure silica (silicon dioxide) uncontaminated

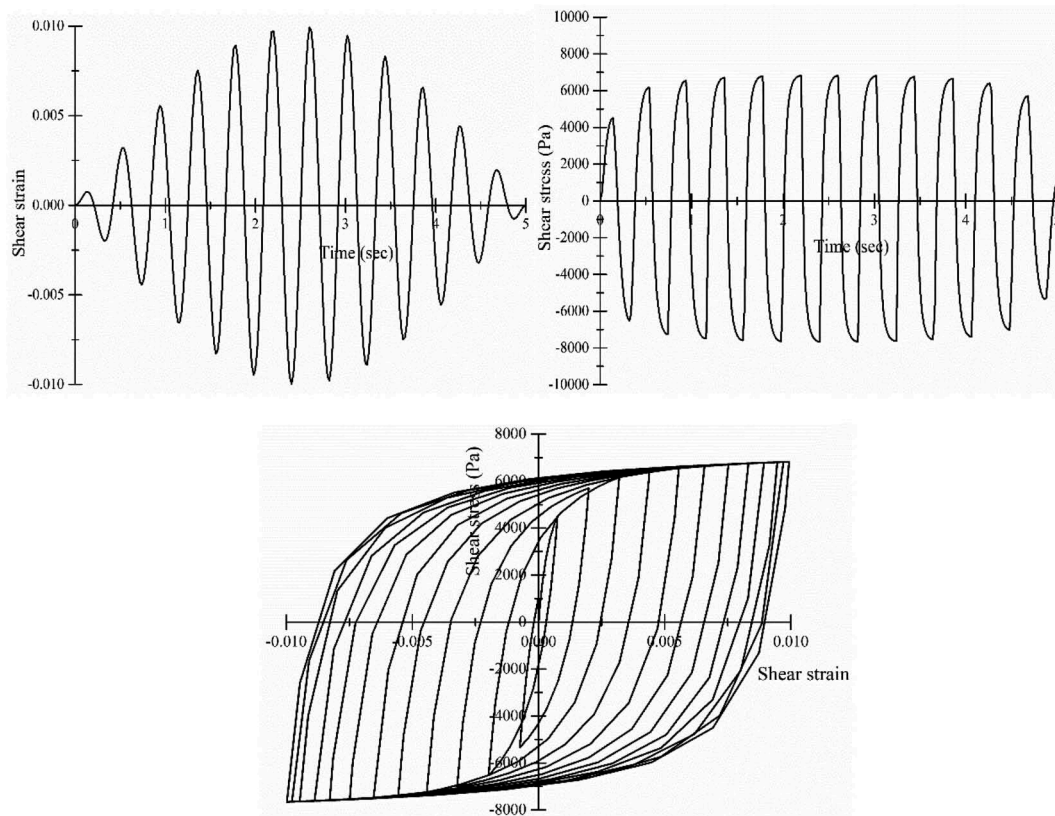


Figure 3. Behaviour of soil column with sinusoidal strain with amplitude ramping up to 1% and then decreasing gradually back to zero.



Figure 4. Geotechnical laminar box test setup.

by clay, loam, iron compounds, or other foreign substances. The maximum and minimum void ratios of the sand are 0.800 and 0.608, respectively (Thevanayagam *et al.* 2003, NEES 2009). The Ottawa sand is pumped into the GLB using hydraulic slurry processes (Coleman *et al.* 2016). The instruments like accelerometers are placed inside the GLB at different depths to enable

measurement of real-time soil shear wave velocity as it propagates through the soil column.

For measurement of real-time shear wave velocity of the soil, the accelerometers are placed at different depths along the depth of the soil column and the first arrival time of the S-wave at each accelerometer is recorded. The time difference between two arrival times for accelerometer is noted and is divided by the distance between them to get its shear wave velocity. This exercise is repeated at each depth to get the profile of shear wave velocity. A schematic diagram illustrating the locations of accelerometers at different depths in the soil is shown in Figure 5 and Table 1. To get the average shear wave velocity profile with depth, more than 25 tests have been conducted at 9 Hz, 8 Hz and 6 Hz input motions with a PGA of 0.03 g. For illustration purpose, the determination of V_s at a depth of 2.849 m is illustrated in the following section.

The entire time history of ACC 18 and ACC 22 is shown in Figure 6(a) above. For finding the arrival time of the waves for each of the accelerometer readings, the enlarged view of the initial portion of the accelerometer reading is shown in Figure 6(b) and the time difference of the wave arrival time is found to be 0.005 sec. The

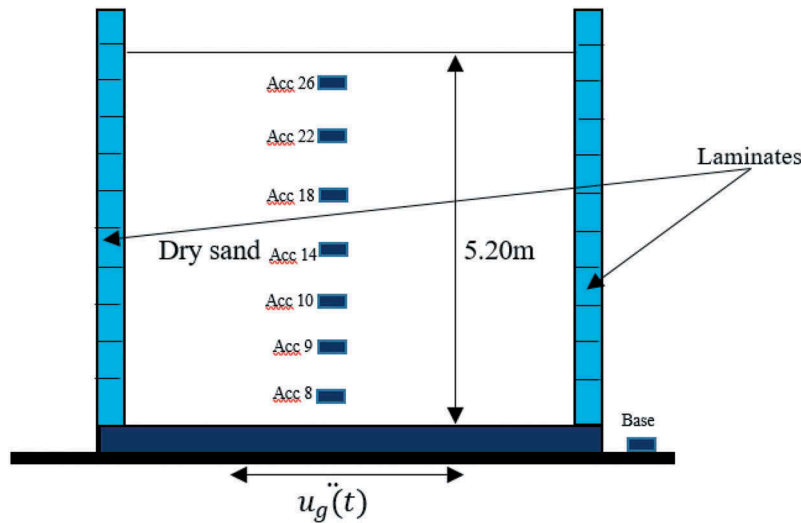


Figure 5. A schematic diagram of soil column in laminar box with accelerometer locations.

Table 1. Locations of the accelerometers within the GLB.

Accelerometers	Height above the base (m)
ACC 26	4.069
ACC 22	3.459
ACC 18	2.849
ACC 14	2.239
ACC 10	1.630
ACC 9	1.020
ACC 8	0.410
Base	0

corresponding shear wave velocity of the soil is found to be $V_s = (3.459 - 2.849) / 0.005 = 122$ m/s. This exercise is repeated for each of the 25 test and an average value of V_s is taken for this depth of the soil.

For getting the entire profile of V_s with depth, the entire process is repeated for each depth of recording and the final shear wave velocity profile with depth of soil is shown in Figure 7. Using the above soil shear wave velocity profile, the numerical models developed during this study are validated with one such base motion chosen which has a peak amplitude of 0.03 g and 9 Hz frequency. The recording of the time history has been done for 12 secs and is shown in Figure 8(a,b) in both time and frequency domains.

The discretisation of the soil column within the laminar box test for the numerical analyses in DEEPSOIL (Hashash *et al.* 2012) and developed program for both equivalent linear and nonlinear analysis is shown in Figure 9. The grid dimensions are selected by considering the maximum frequency (f_{max}) of the shear wave that the model could logically respond to during earthquake loadings (Kuhlemeyer and Lysmer 1973). To capture the strain-dependant dynamic properties of F-55 Ottawa sand which will be utilised in the equivalent linear and nonlinear soil model, torsional

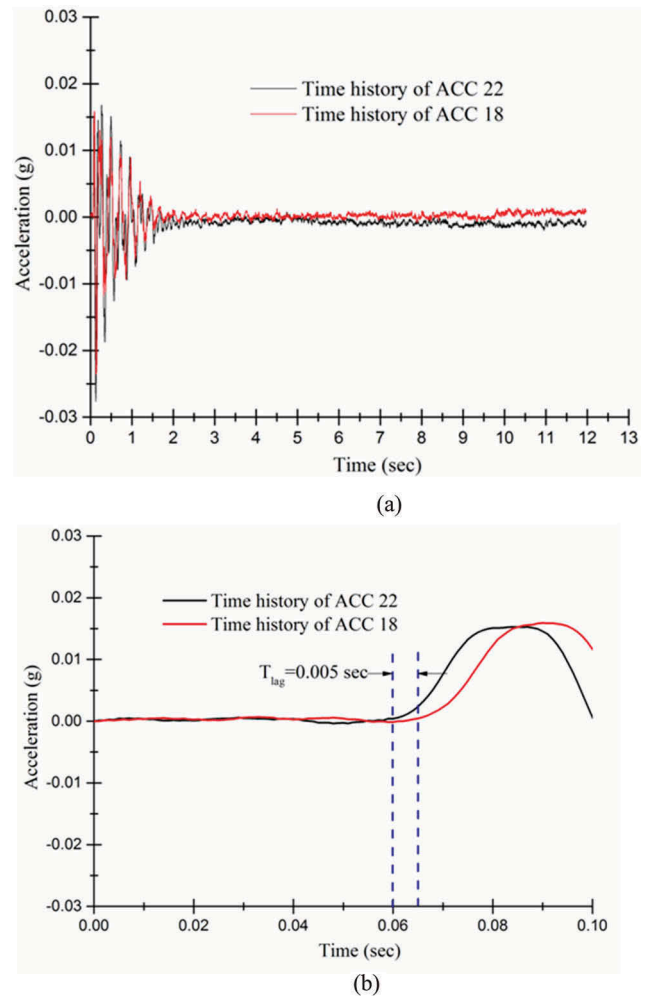


Figure 6. (a) Recorded time history of ACC 18 and ACC 22 in laminar box test. (b) Enlarged view of the recorded time history of ACC 18 and ACC 22.

resonant column laboratory test (RCT) is conducted on the same soil sample for two different confining

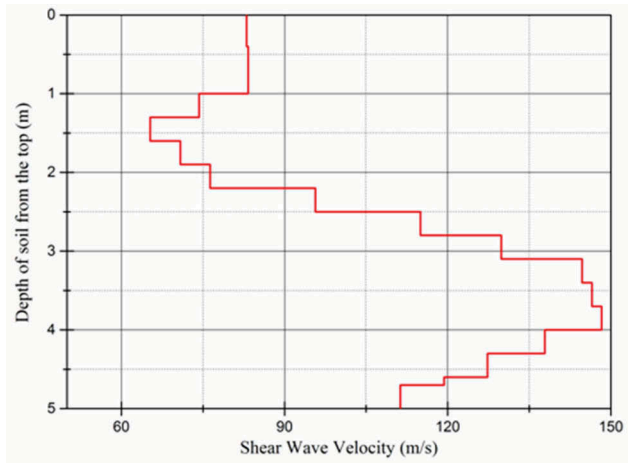
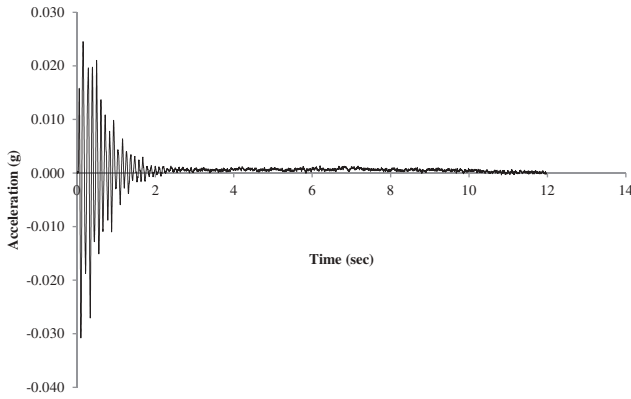
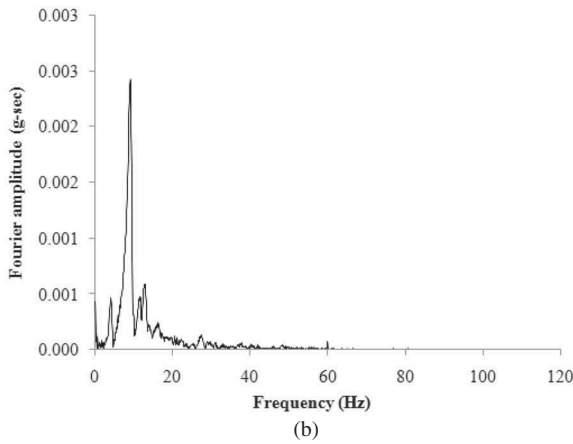


Figure 7. Shear wave velocity of soil with depth of soil in a laminar box test.



(a)



(b)

Figure 8. Applied base motion to the laminar box in both (a) time and (b) frequency domain.

pressures (13.8 kPa and 55.16 kPa). The tests are done on a soil sample of 10.77 cm in height with an initial diameter of 5.07 cm. The type of sand is SP and its relative density is 58%. The specific gravity of sand is 2.65 with an initial void ratio of 0.61. The dry unit

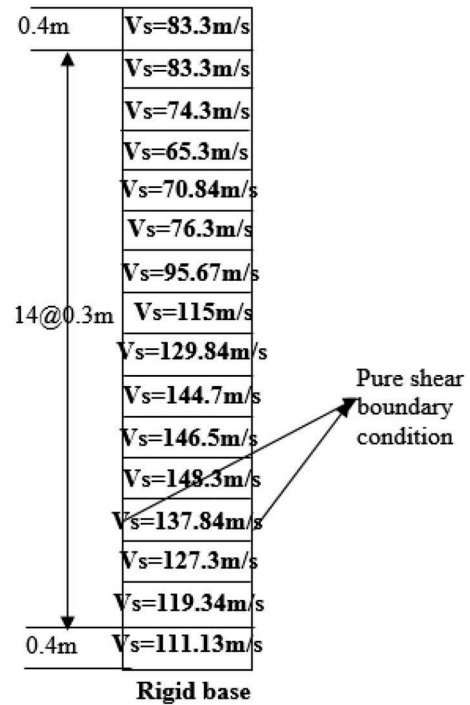


Figure 9. Numerical discretisation of soil column in GLB test.

weight of the sand is 15.90kN/m³. The experimental curves of the normalised stiffness and its corresponding damping ratio of the Ottawa sand are shown in Figure 10(a,b). The curve fits of the experimental data for both normalised stiffness (G/G_{max}) and damping ratio (D) are given in Equations (12–15) below for two different confining pressures,

$$\frac{G}{G_{max}} = \frac{1.005}{(1 + \exp((-(\log_{10}\gamma) + 1.479) / -0.4492))},$$

for confining pressure of 13.8kPa (12)

$$\frac{G}{G_{max}} = \frac{1.005}{(1 + \exp((-(\log_{10}\gamma) + 1.229) / -0.4492))},$$

for confining pressure of 55.16kPa (13)

$$D(\%) = 0.1514 + \frac{0.2733451}{(1.85 + \exp((-3.8597 * ((\log_{10}\gamma) + 1.2882))))},$$

for confining pressure of 13.8kPa (14)

$$D(\%) = 0.15014 + \frac{0.2833451}{(3.05 + \exp((-3.8597 * ((\log_{10}\gamma) + 1.1082))))},$$

for confining pressure of 55.16kPa (15)

These equations are useful for the calibration of backbone curve which will be utilised for nonlinear analysis of soil. For generating the backbone curves of the top 2 m of the soil, the normalised stiffness

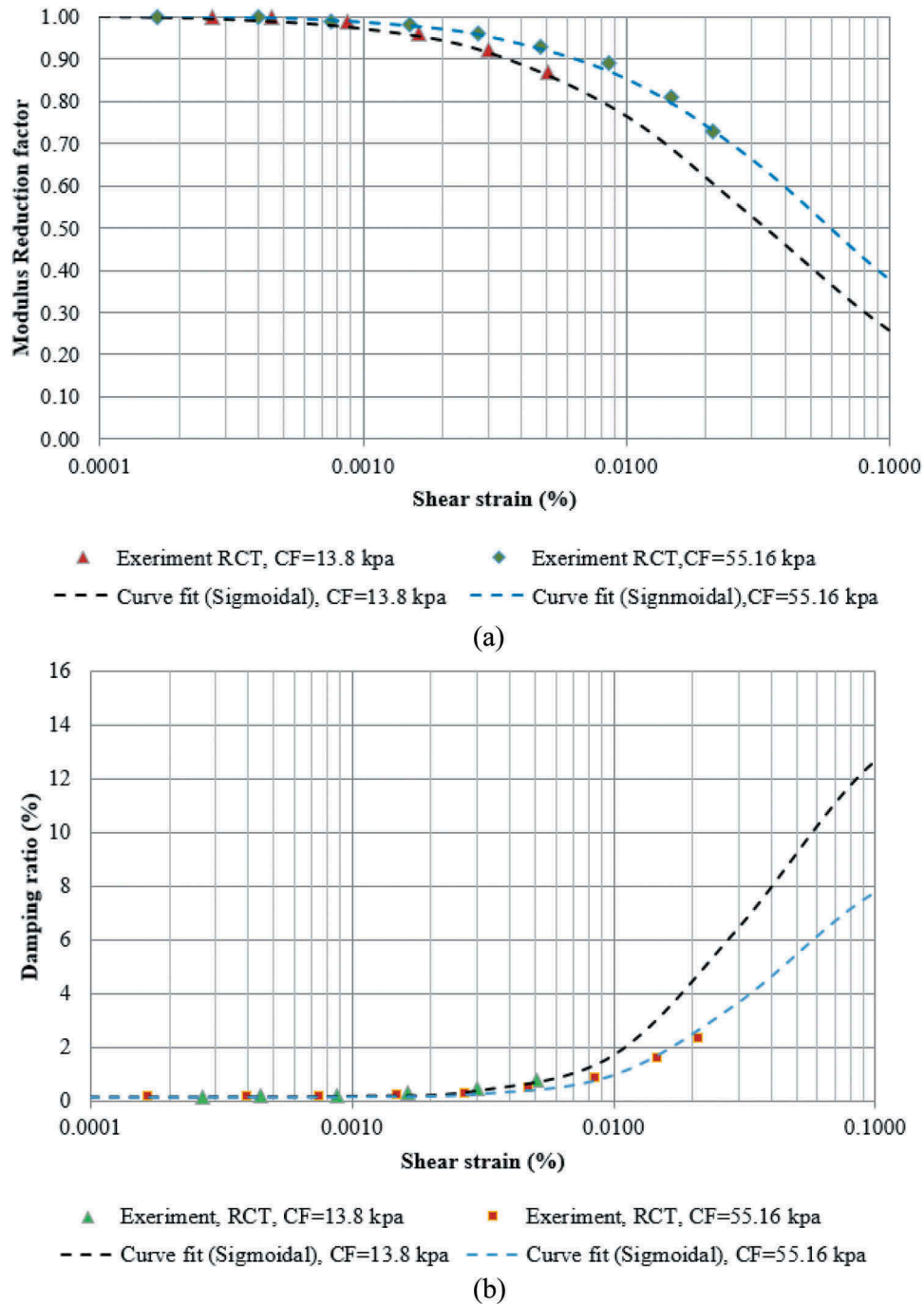


Figure 10. Variation of (a) normalised stiffness and (b) damping ratio versus shear strain for F-55 Ottawa sand by torsional resonant column tests (RCT).

and damping ratio is assigned for a confining pressure of 13.8 kPa, and the rest is assigned for a confining pressure of 55.16 kPa. These observations are based on the equivalence of the average confining stresses on these layers.

4. Calibration of the backbone curve from strain-dependant properties of soil

The hysteretic form of the Kelvin–Voigt model consists of a spring (of shear modulus G) and a dashpot (of viscosity η) connected in parallel (Kramer 2005). Thus, the strain, γ , is imposed equally on the two elements and

the corresponding stress, τ , has two components, one acting on the spring, $\tau_{\text{spr}} = Gu(t)$ and another one on the dashpot, $\tau_{\text{damper}} = \eta \dot{u}(t)$, where $u(t)$ is the shear strain of the soil. Combining these two resistances, the final expression for stress is given as,

$$\tau(t) = Gu(t) + \eta \dot{u}(t) \quad (16)$$

For a harmonic excitation of the form, $F(t) = F_o \sin(\omega t)$, the response (in terms of displacement) is also of the form $u(t) = u_o \sin(\omega t)$ and the velocity is $\dot{u}(t) = \omega u_o \cos(\omega t)$. The final expression may be expressed as,

$$\begin{aligned} \left(\frac{u(t)}{u_o}\right)^2 + \left(\frac{\dot{u}(t)}{\omega u_o}\right)^2 &= 1 \\ \text{Or, } \left(\frac{\dot{u}(t)}{\omega u_o}\right)^2 &= 1 - \left(\frac{u(t)}{u_o}\right)^2 \\ \text{Or, } \left(\frac{\dot{u}(t)}{\omega u_o}\right) &= \pm \sqrt{1 - \left(\frac{u(t)}{u_o}\right)^2} \\ \text{Or, } \dot{u}(t) &= \pm \omega \sqrt{u_o^2 - u(t)^2} \end{aligned} \quad (17)$$

Substituting, Equation (17) into Equation (16), the following expression for shear stress may be obtained,

$$\tau(t) = Gu(t) \pm \eta \omega \sqrt{u_o^2 - u(t)^2} \quad (18)$$

where '+' is for the re-loading and '-' is for the unloading.

In the above equation, the term ' $\eta\omega$ ' is replaced by ' $2G\xi$ ' to make the expression frequency independent. Thus, Equation (18) may be expressed as,

$$\tau(t) = Gu(t) \pm 2G\xi \sqrt{u_o^2 - u(t)^2} \quad (19)$$

The above expression will give an ellipse for a value of shear modulus (G) and damping ratio (ξ). To incorporate strain dependency of shear modulus and damping ratio into Equation (19), the equation may be modified as,

$$\tau(t) = G(u_o)u(t) \pm 2G(u_o)\xi(u_o)\sqrt{u_o^2 - u(t)^2} \quad (20)$$

where u_o is the amplitude of the shear strain. $G(u_o)$ and $D(u_o)$ are obtained from the curves of modulus reduction and damping ratio with shear strain. This equation gives the equivalent hysteretic hypothesis using the strain dependant Kelvin–Voigt model. Equation 20 is used to define an appropriate linear soil column model of 1 m height with a value of small strain shear modulus. An in-house code is developed in which the base of the soil column is fixed and at the top of the soil, a sine wave of constant amplitude of strain is applied. The response is in the form of shear stress which produces an inclined ellipse with amplitude of strain. The exercise is repeated for all the shear strain amplitudes (ranging from $10^{-4}\%$ to 0.1%). Figure 11 shows the hysteresis loops for each model data point based on the equivalent linear model data. Figure 11 also shows the backbone curve (in blue) which is used for the nonlinear model shear stress versus shear strain curve. The equation of backbone curve (Modified MKZ model as per Hashash and Park

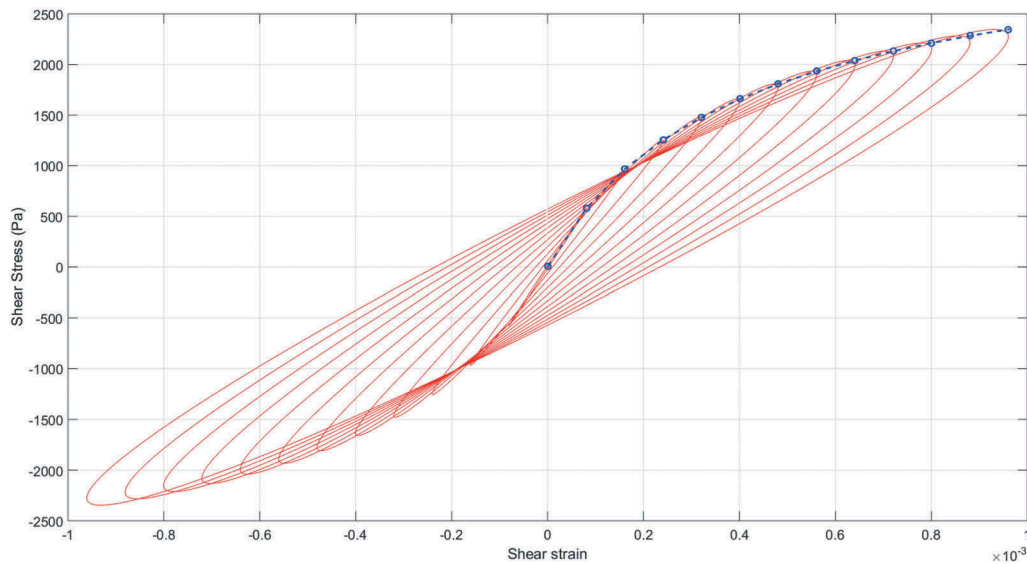


Figure 11. Variation of shear stress with shear strain in soil in a strain-dependent linear Kelvin–Voigt model.

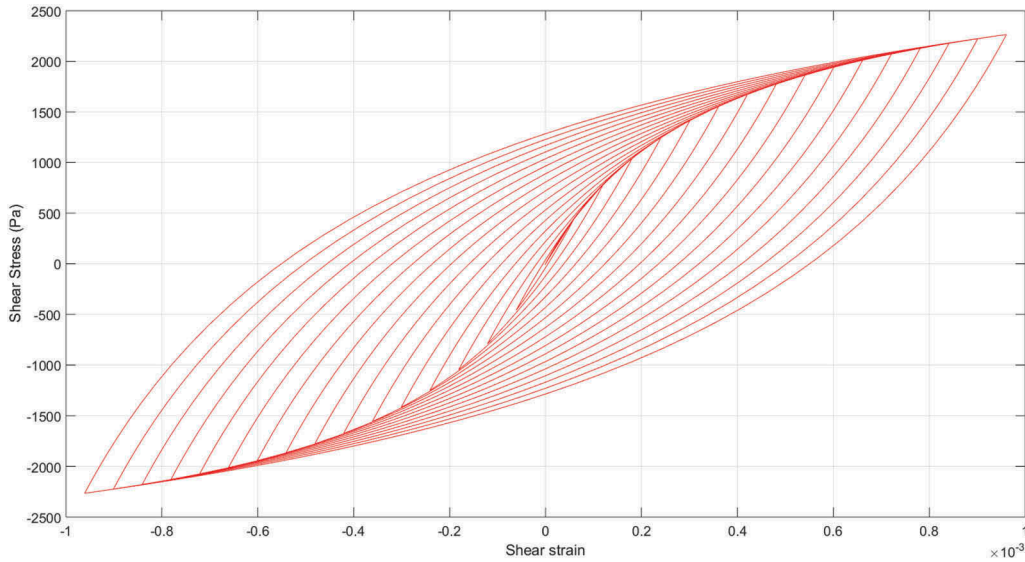


Figure 12. Variation of shear stress with shear strain in soil following the first two Masing rules.

(2002) to be used in the non-linear analysis of sandy soil is given by Equation (21)

$$\tau(t) = \frac{Gu(t)}{1 + \beta \left(\frac{u(t)}{u_{ref}} \right)^s} \quad (21)$$

where $\beta = 1.59$, $s = 0.66$ and $u_{ref} = 0.00092$ for a sandy soil. Using the equation of the backbone curve with the above parameters, a code is developed which considers the unloading and reloading portions of the non-linear loops using the first two Masing rules (Masing 1926). Essentially, these state that (1) a new (but inverted) function is started upon reversal, implying that the initial unload modulus is G , and (2) the first quarter-cycle of loading is scaled by one-half relative to all other cycles (Itasca 2005). The stress-strain curve following the Masing rules is shown in Figure 12. The material properties for the nonlinear model are defined to match the equivalent linear material properties (shown in Figure 13(b)) as close as possible in terms of modulus reduction. The energy absorption for the lowest strain value (shown in Figure 13(b)) is approximated by adding a lower strain damping to the nonlinear model material properties. The calibration of the model in terms of the modulus reduction of a sandy soil with strain is shown in Figure 13(a). Though the match with modulus reduction curve is good, a deviation may be noticed in the damping ratio at higher strain levels (refer to Figure 13(b)). Similar observation is noticed in FLAC2D (Itasca 2005). An overestimation of the damping response at large strains results from the Masing second rule. Even if one modifies the second rule (following Cundall-Pyke rules), there will not be

any significant decrease in the damping ratio at large strains.

At large strains, the soil shear strength is reached and the loops become smaller in area (it is always recorded experimentally). The present hyperbolic soil model does not incorporate ‘strength correction’, that is, there is no cut off for shear strength at large strains (there is continuous increase in shear stress with strain) due to which the area of the loop is more than the recorded (experimental) values. Hence, the damping ratio is more at large strains.

This leads to an underestimation of shear strains as well as surface intensities in the form of PGA at the ground surface. The energy absorbed per cycle for the soil column is calculated as the area of the hysteresis loop for each amplitude of shear strain. Equation 22 shows a simple trapezoid rule for numerical integration that may be used if the shear stress and the shear strain are in tabular form (Spears and Coleman 2015),

$$E_{loop} = \sum_{j=1}^N \frac{\tau_j + \tau_{j-1}}{2} (u_{oj} - u_{oj-1}) \quad (22)$$

The final parameters of the backbone curve for the F-55 Ottawa sand is given in Table 2. After calibration with the stiffness degradation only disregarding the mismatch with the damping values at higher strains, the value of γ_{ref} (the reference shear strain) used for the hyperbolic model in Equation (11) is found to be 0.059% and 0.0345% for confining pressures of 13.8 and 55.16 kPa, respectively. These backbone curves are used for the nonlinear analysis of F-55 Ottawa sand in laminar box tests. It is also validated against the results obtained from DEEPSOIL (Hashash *et al.*

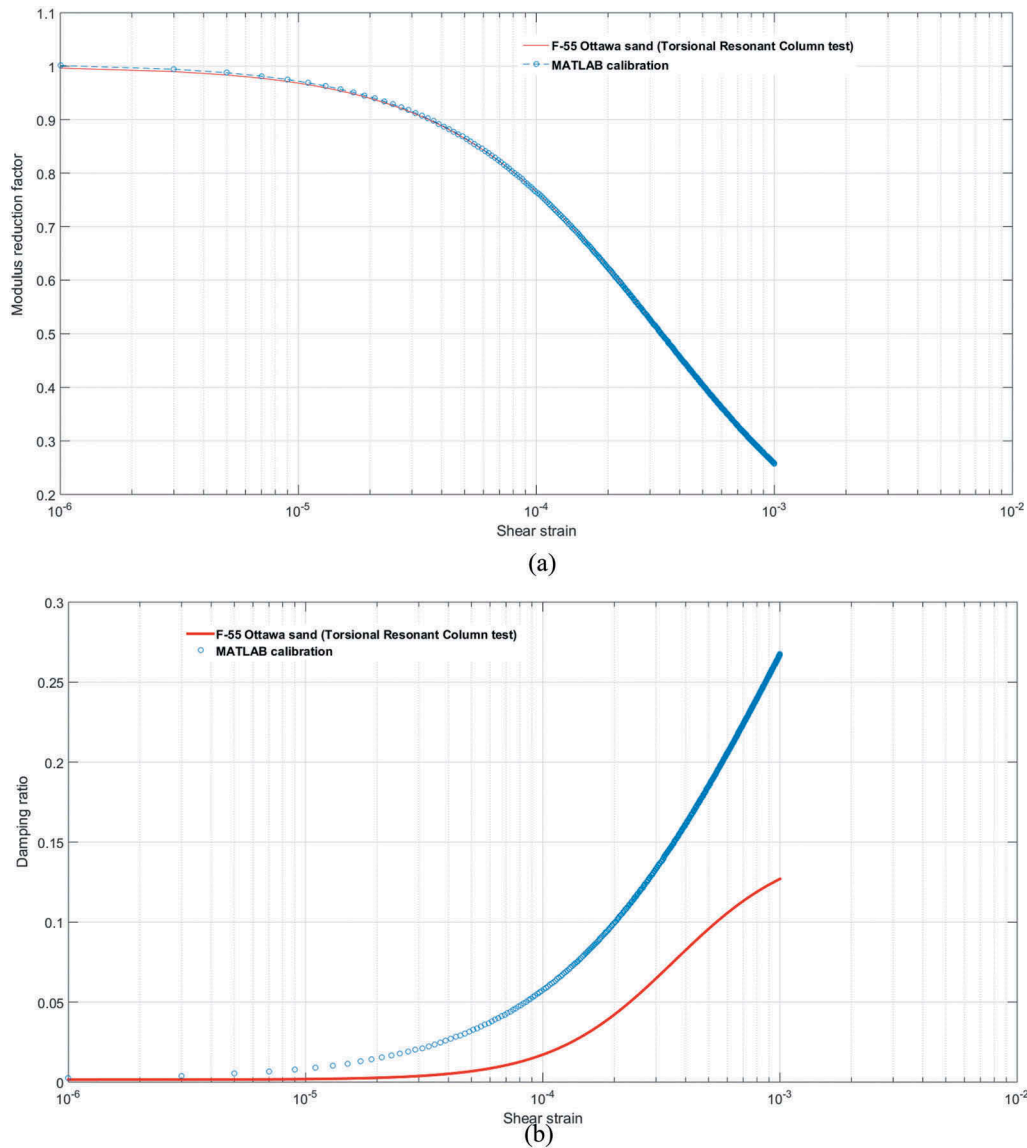


Figure 13. (a). Comparison of shear modulus reduction with strain obtained from MATLAB and that found in F-55 Ottawa sand. (b). Comparison of damping ratio with strain obtained from MATLAB and that found in F-55 Ottawa sand.

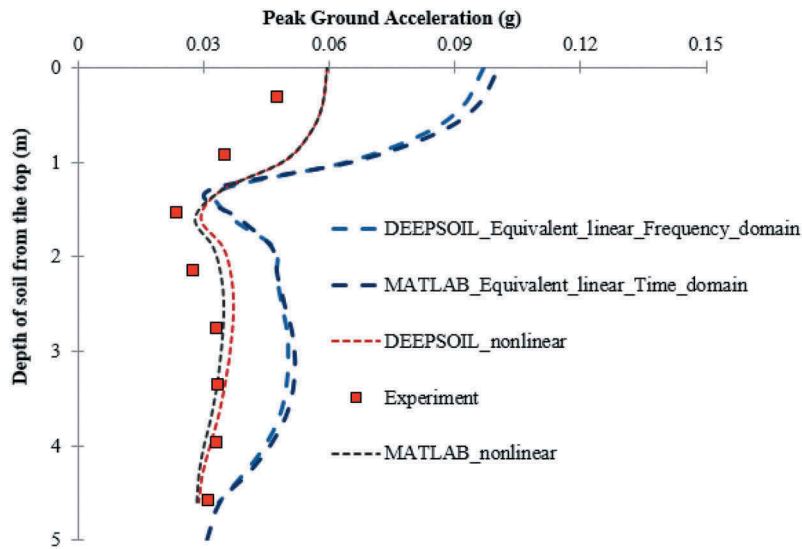
Table 2. The curve fit parameters for F-55 Ottawa sand.

Type of Soil	β value	s value	u_{ref}
F-55 Ottawa Sand (CF = 13.8 kPa)	1.52	0.976	0.000515
F-55 Ottawa Sand (CF = 55.16 kPa)	1.46	0.975	0.00088

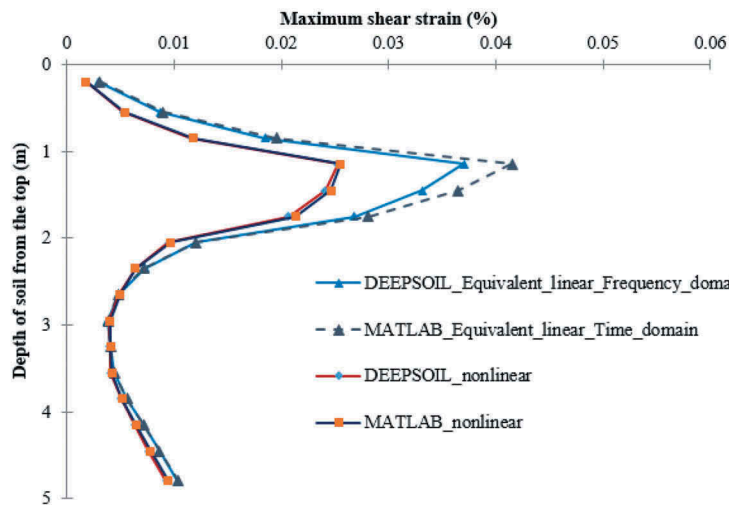
2012). The small strain damping used for the non-linear analysis is taken to be 4%. This value seems to be quite high but it was required to reduce the artificial noise in the response.

The experimental validation of the developed model is shown in terms of variation of acceleration with depth for the specified base motion in Figure 14 (a). The model predictions (equivalent linear and nonlinear) are compared with the test results and results obtained from DEEPSOIL (Hashash *et al.*

2012) program. In addition, the numerical validation of shear strain with depth obtained from DEEPSOIL is compared with the developed models which is shown in Figure 14(b). From Figure 14(a), it is observed that there is a drop in the peak acceleration value around 3 to 4 m depth. This is because of an interference of second mode of vibration in the soil column during the test which has a lesser amount of mass participation in comparison to its fundamental mode. This observation is also supported by comparing the acceleration time history in the frequency domain, both numerically and experimentally, for ACC 8 and ACC 14 (refer to Figure 15). Moreover, in comparison to equivalent linear analysis, the non-linear analysis predicts closer results in terms of PGA with depth with the experimental observations. From



(a)



(b)

Figure 14. Comparison of the (a) peak accelerations and (b) Maximum shear strain with soil column depth in the GLB test for equivalent linear and nonlinear analysis.

the Fourier spectrum of ACC8 and ACC 14, it may be seen that there are three predominant peaks, the first one at 4.26 Hz, second one at 9 Hz and the final one at 12.56 Hz. Out of these, the peak at 9 Hz is the frequency of the input motion, and the peaks at 4.26 Hz and 12.76 Hz are the two fundamental modes of vibration of the soil column. Hence, the notion that the higher modes are occurring during the experiment is supported by these findings which also supports the fact of the de-amplification of peak accelerations as observed in Figure 14(a). The results obtained from the numerical analysis are close to the experimental observations and demonstrate the numerical predictive capability of the developed model in equivalent linear and nonlinear domain.

The deformations of the soil column at two instants of time obtained from the developed program for equivalent linear analysis are shown in Figure 16. From the deformed mesh at 0.15 sec, it may be observed that there is an influence of higher modes along with the fundamental modes of the soil column, which is dominant at a height of around 3–4.5 m. This is not observed in the deformed mesh at 0.075 sec in which the entire soil column is moving in its fundamental mode. This is also a supportive evidence of the de-amplification of peak acceleration at the concerned zone as shown in Figure 14(a). The small differences are due to the frequency domain technique utilised in DEEPSOIL (Hashash *et al.* 2012) and the time domain technique

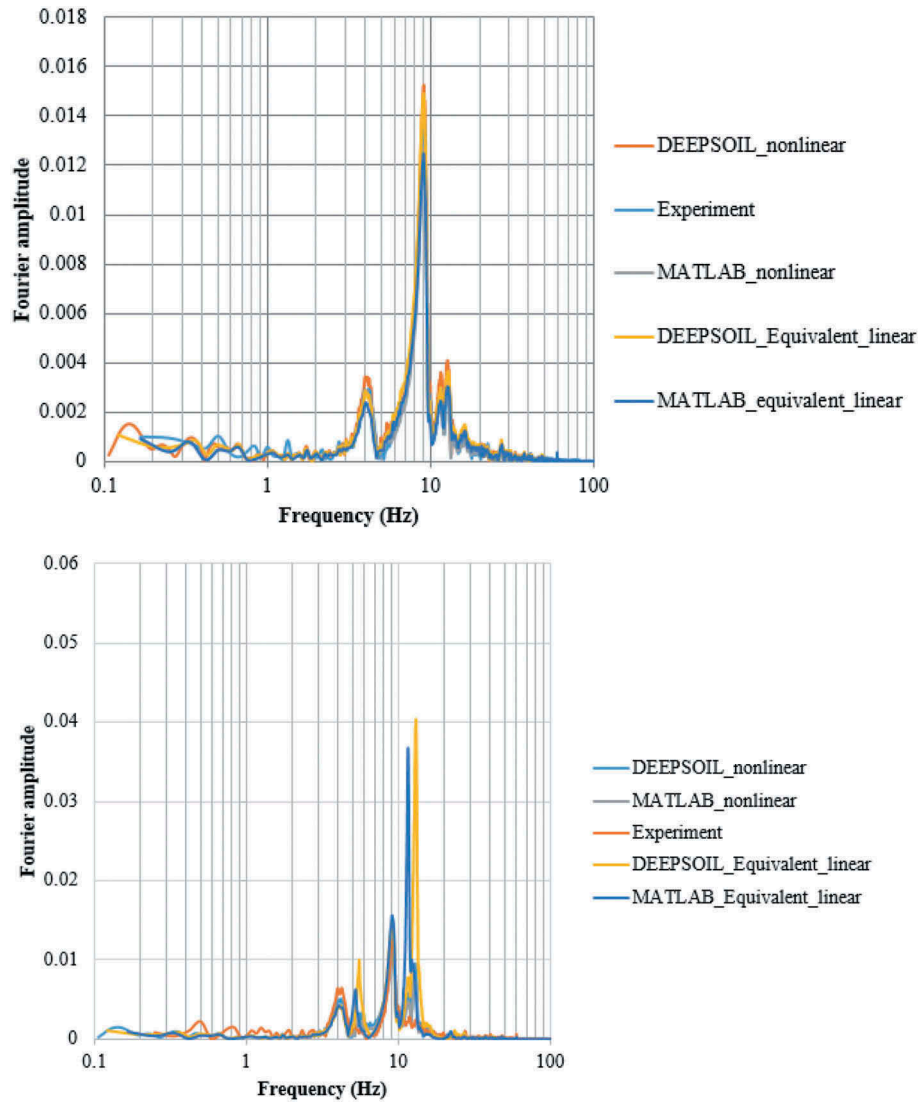


Figure 15. Fourier spectrum of ACC8 and ACC14 from GLB experiments MATLAB and DEEPSOIL.

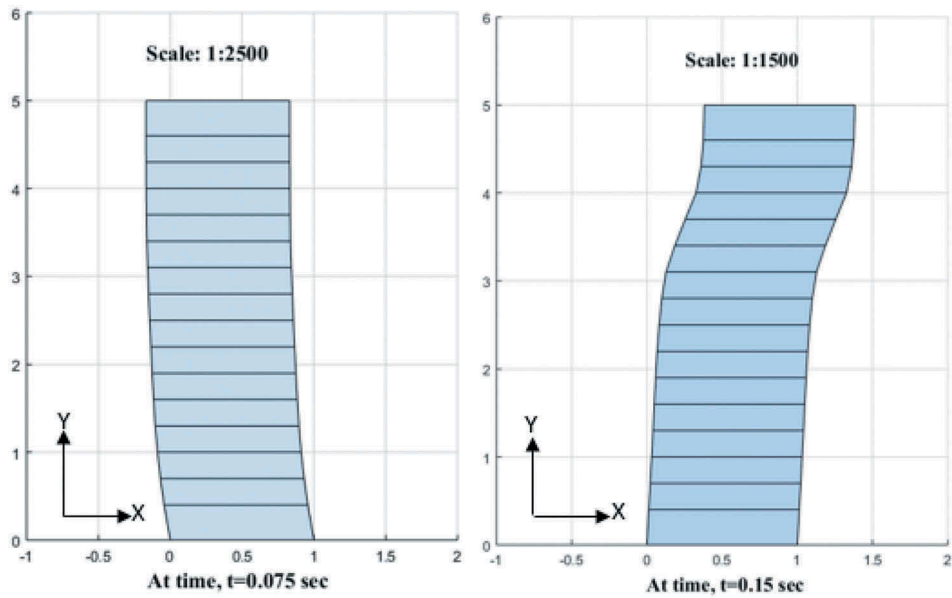
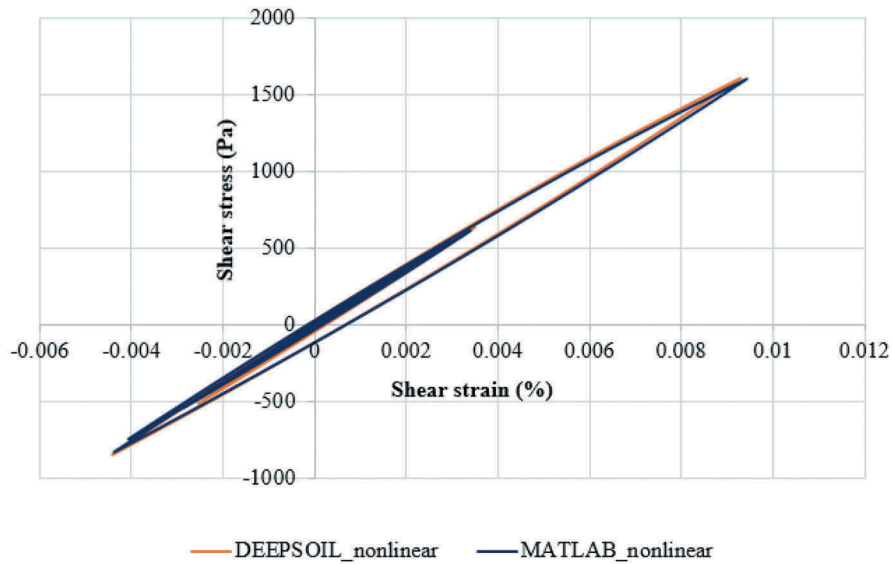
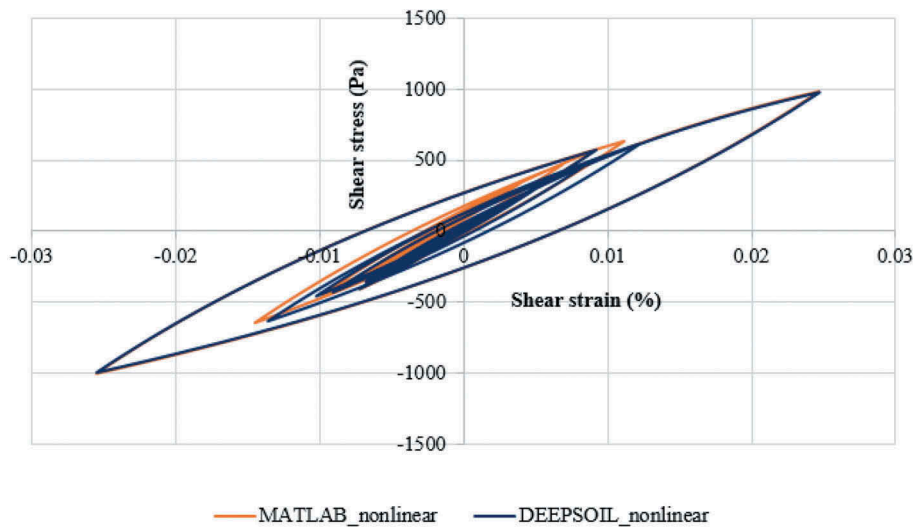


Figure 16. Deformations of the soil column at two time instants predicted by MATLAB program.



(a)



(b)

Figure 17. Comparison of stress-strain loops for soil column at a depth of (a) 5 m (b) 1.3 m from the top of the soil surface.

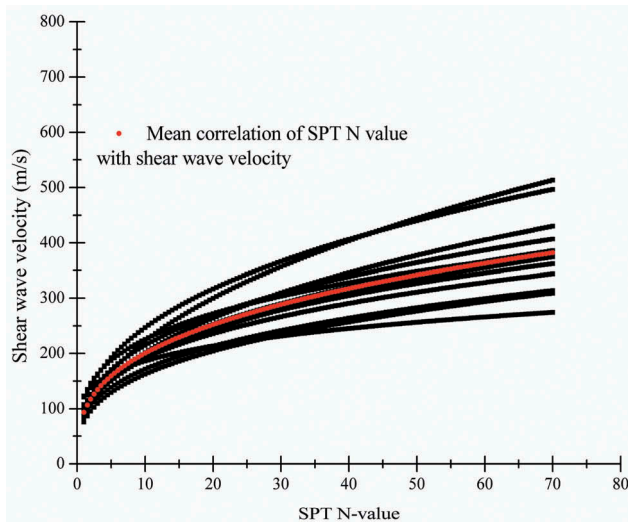
(Newmark's β -method) utilised in the developed model to solve the same problem in equivalent linear domain. To validate the correctness of the stress-strain rules for nonlinear analysis, the shear stress vs. shear strains have been compared with DEEPSOIL and the developed code at depths of 5 m and 1.3 m from the top of the soil surface (refer to Figure 17). It is seen that the stress-strain loops match reasonably well for depths of 1.3 m and 5 m. Thus, these results validate the nonlinear code which is further used for the prediction of the behaviour of two sites in Mumbai.

5. Nonlinear site response analysis of Mumbai sites and its comparison with equivalent linear response

In the present study, field borehole log data consisting of variation of SPT N-value with the depth of soil of two sites in Mumbai city are considered for the analyses. Often the shear wave velocity (V_s in m/s) of the soil is obtained by the correlation with the field standard penetration test (SPT) N-values in absence of proper dynamic field test data. A correlation between shear wave velocity (V_s) and SPT N-value for various soil profiles of

Table 3. Correlations of SPT N-value with the shear wave velocity of soil.

Correlation	Reference
$V_s = 76N^{0.33}$	Imai and Yoshimura (1970)
$V_s = 82N^{0.39}$	Ohsaki and Iwasaki (1973)
$V_s = 91N^{0.337}$	Imai and Yoshimura (1970)
$V_s = 90N^{0.34}$	Imai and Yoshimura (1970)
$V_s = 100.5N^{0.329}$	Sykora and Stokoe (1983)
$V_s = 107.6N^{0.36}$	Athanasopoulos (1995)
$V_s = 116.1(N + 0.3185)^{0.202}$	Jinan (1987)
$V_s = 82.6N^{0.43}$	Hanumanthrao and Ramana (2008)
$V_s = 95.64N^{0.301}$	Maheshwari <i>et al.</i> (2010)

**Figure 18.** Variation of shear wave velocity of soil with N-value for Mumbai city.

Mumbai city has been developed using various published correlations for sand and clay as shown in Table 3. The correlation thus developed is utilised

for the site response analyses. The average value of these calculated shear wave velocities is used in the present study. A nonlinear regression analysis employing power model has been implemented using the SPT N-values with average shear wave velocity (V_s) for the soils and shown in Figure 18. The obtained best fit relationship of shear wave velocity with SPT N-value for the city of Mumbai is given by,

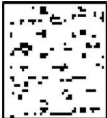
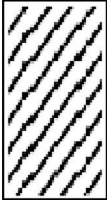
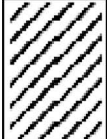
$$V_s \left(\text{in } \frac{m}{s} \right) = 93.34(N)^{0.33162} \quad (23)$$

The field borehole data from two sites in Mumbai, namely Site-1 and Site-2, have been used for the present analyses. The borehole log for the above two sites are presented in Tables 4 and 5. The bedrock, located at 7.5 m depth, is considered as rigid and hence energy dissipation due to the reflection of seismic waves at the bedrock/soil boundaries is not considered. A typical borehole log detail (for Site-2) is shown in Figure 19 which shows the layer depths and depth of bedrock as well as the measured soil properties. A real ground (rock motion, as the bedrock is located at a shallow depth in Mumbai) motion is chosen in such a way that its frequency content matches with the predominant period of the sites in Mumbai, which typically lies between 0.1 and 0.3 s. The 1979 Imperial Valley Earthquake motion is selected based on the frequency contents and spectral compatibility with the Indian building code (IS:1893(Part 1) 2002) and shown in Figure 20(a). As the city of Mumbai lies in Zone-III as per Indian Building code, the PGA for this zone is 0.16 g, hence the selected motion has been

Table 4. Soil profile and their properties at site-1 in Mumbai.

SITE-1	Type of soil	Depth of soil	SPT N-value	Shear wave velocity (m/s)
	Black clayey SAND with gravels	(0.0–0.50)m	12	212.78
	Dense silty SAND with gravels	(0.5–3.25)m	29	285.12
	Very dense silty SAND with gravels	(3.25–4.50)m	30	288.35
	Very stiff silty CLAY with gravels	(4.5–7.50)m	24(PI = 24)	267.77

Table 5. Soil profile and their properties at site-2in Mumbai.

SITE-2	Type of soil	Depth of soil	SPT N-value	Shear wave velocity (m/s)
	Black clayey SAND	(0.0–0.50)m	12	212.78
	Stiff highly compressible CLAY	(0.5–3.25)m	15(P _I = 42)	229.13
	Very stiff highly compressible silty CLAY	(3.25–6.25)m	19(P _I = 42)	247.81
	Hard highly compressible silty CLAY	(6.25–7.50)m	30 (P _I = 14)	288.35

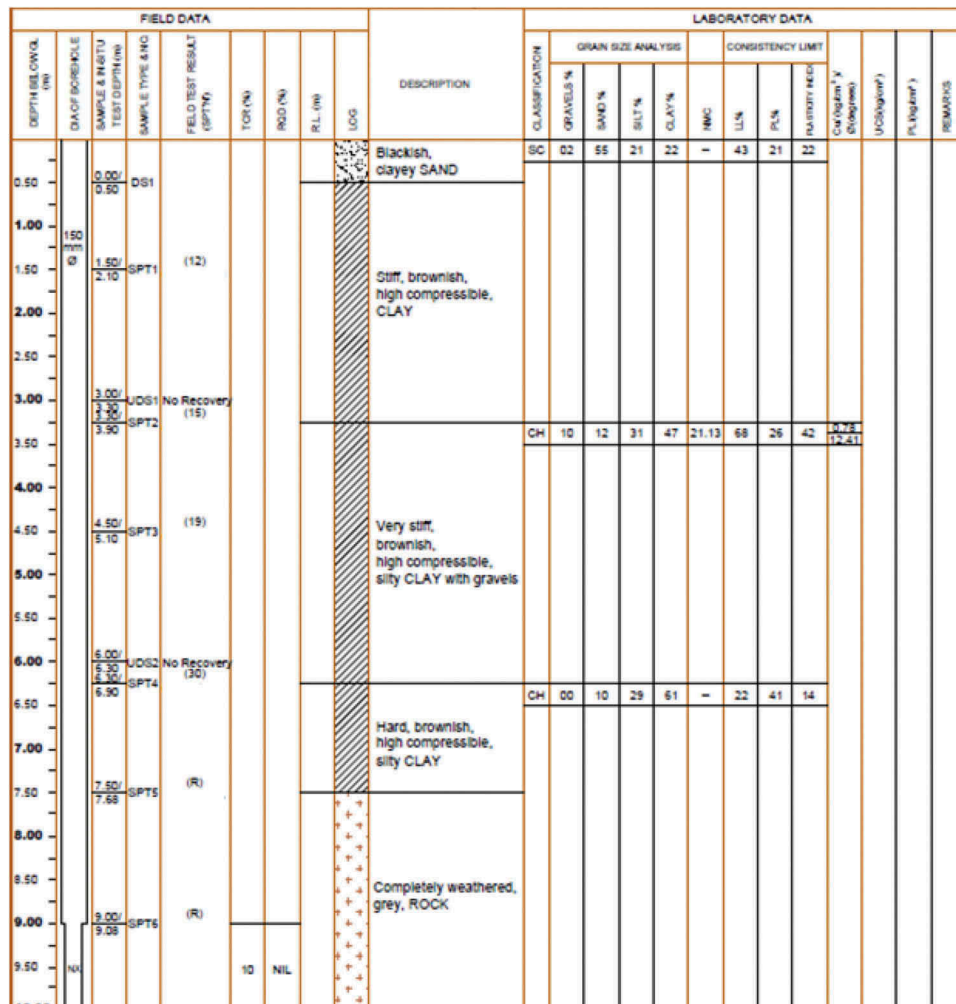


Figure 19. A typical borehole log (for Site-2) of Mumbai city.

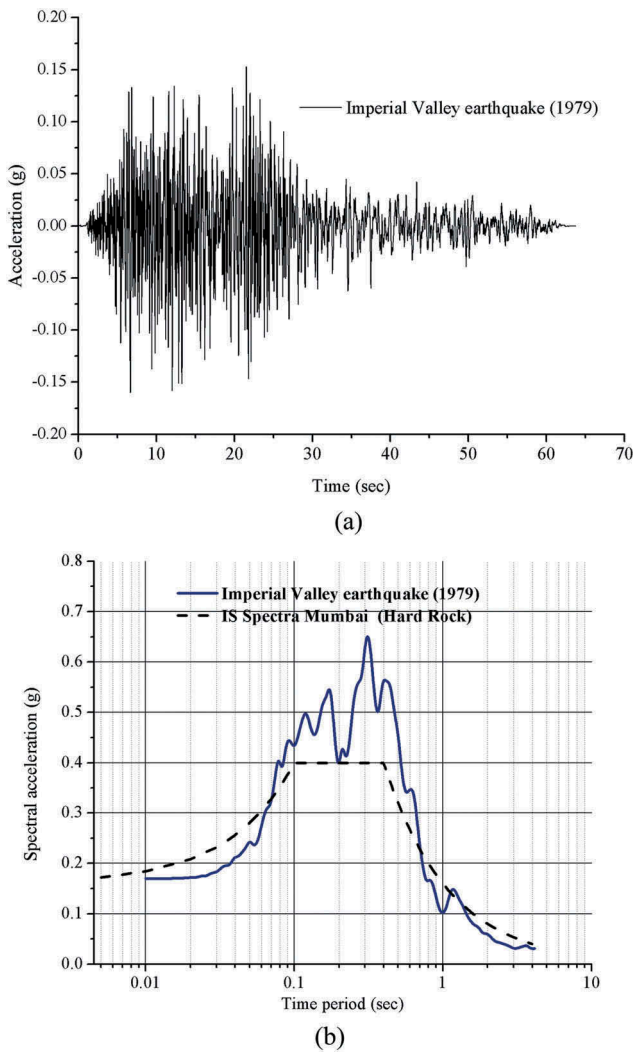


Figure 20. (a). Selected earthquake motion (1979 imperial valley earthquake). (b). Comparison of Indian building code (IS:1893 (Part 1) 2002) response spectra with 1979 imperial valley earthquake spectra.

arithmetically scaled to PGA of 0.16 g. This PGA value represents the maximum credible earthquake (MCE) for the region. The maximum acceleration (a) and velocity (v) are 160.00 cm/s^2 and 10.95 cm/s for 1979 Imperial Valley Earthquake. Thus, the ratio of the velocity and the acceleration is 0.0684, which is less than 0.1 confirming it a rock motion (Newmark 1965). A comparison between the response spectra for hard rock (at 5% damping) at Mumbai from Indian building code (IS:1893 (Part 1) 2002) and the spectra of the selected ground motions are shown in Figure 20(b). From Figure 20(b), it may be seen that the Imperial Valley Earthquake (1979) is conservative between time periods of 0.065 sec to 0.7 sec, which serves the purpose and thus, it is selected for studying the responses of the

sites in Mumbai. For sand and clay layers at the sites, the average G/G_{\max} and D curves developed by (Seed and Idriss 1970, Vucetic and Dobry 1991) are utilised in absence of specific data on Mumbai soils and these backbone curves are shown in Figure 21.

To perform time domain non-linear analysis for Site-1 and Site-2, proper calibration of non-linear soil parameters has been performed before the analysis as per the procedure described previously to find out the parameters of the backbone curve for clay and sandy soil. The calibrated curves from the present study as well as the curves from the literature are compared in Figure 22(a–d). It is observed that there is a very good match between the modulus reduction curves, but there is an over-prediction of damping ratio at large strains. Using the above two backbone curves for clay and sandy soil strata, a nonlinear time domain analysis is performed for Site-1 and Site-2. The numerical discretisation of the soil columns for Site-1 and Site-2 in Mumbai are shown in Figure 23. The base of the soil column is considered infinitely stiff. The soil response is modelled using a modified hyperbolic model as shown by Equation (11) with extended Masing criteria to represent hysteretic loading and unloading of soils. The responses of the two sites in terms of peak acceleration and peak shear strain with depth are obtained by the equivalent linear analysis developed in time domain and compared with the corresponding results from non-linear analysis. It may be also noted that the amplification of motion for the Imperial Valley Earthquake base motion is about 2.95 and 2.88 at Site-1, 3.55 and 2.84 at Site-2 in Mumbai obtained from equivalent linear and non-linear analysis, respectively. The distributions of peak shear strain and PGA with depth at Site-1 and Site-2 are shown in Figure 24(a,b). The figure shows that there is a sudden change in peak strain at 0.5 m and 4.5 m for Site-1 and at 0.5 m, 3.25 m and 6.25 m for Site-2 from both the analyses. This is due to a sudden change in soil properties (change in shear wave velocity, plasticity index of soil, etc.) at these depths. The maximum strain experienced at Site-1 and Site-2 from the non-linear analysis is 0.051% and 0.069%, respectively. The peak shear-strains obtained from the equivalent linear analysis is less, especially in the lower layers of the soil profile where the shear strains are the largest. In the equivalent linear method, it accounts for the nonlinearity by decreasing the shear modulus based on the effective strain. To check whether the PGA at the ground surface

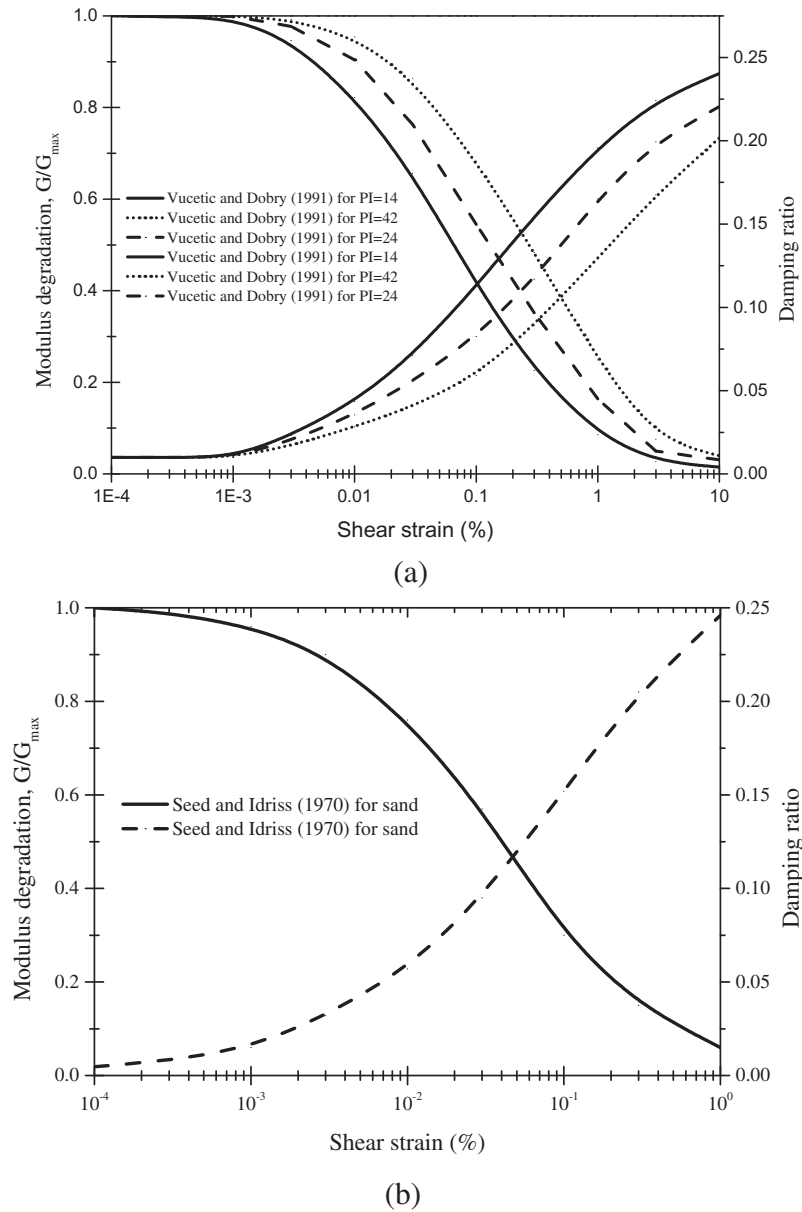


Figure 21. G/G_{\max} and damping ratio (D) curves for (a) sand and (b) clay with different plasticity index.

obtained by this analysis is realistic or not, the values obtained by the analyses are compared with the ordinates of the response spectrum of Imperial Valley Earthquake (1979) corresponding to the natural frequency of Site-1 (9.08 Hz) and Site-2 (8.12 Hz). The ordinates corresponding to the natural frequency of Site-1 and Site-2 are 0.478 g and 0.497 g, respectively. The PGA values predicted by the equivalent linear and non-linear analyses at Site-1 are 0.50 g and 0.48 g, for Site-2 and 0.61 g and 0.478 g, respectively. Thus, the PGA values are over-predicted by the equivalent linear method. This highlights the limitation of the equivalent linear analysis. From Figure 24, it is observed that the nonlinear PGA values

are not always less than the equivalent linear at all the depths of soil column. They can be higher due to the generation of high-frequency contents which can be real or artificial as the nonlinear analysis has a tendency of reproducing high-frequency component in the response spectra. The artificial high-frequency components originate because there is a sudden change in stiffness from unloading to reloading which occurs after each cycle of deformation and sometimes, it happens that there are higher modes which gets excited in non-linear analysis. For a harmonic nature of shear strain, if the shear stress is anything other than harmonic then it leads to a variety of high frequency in addition to the input

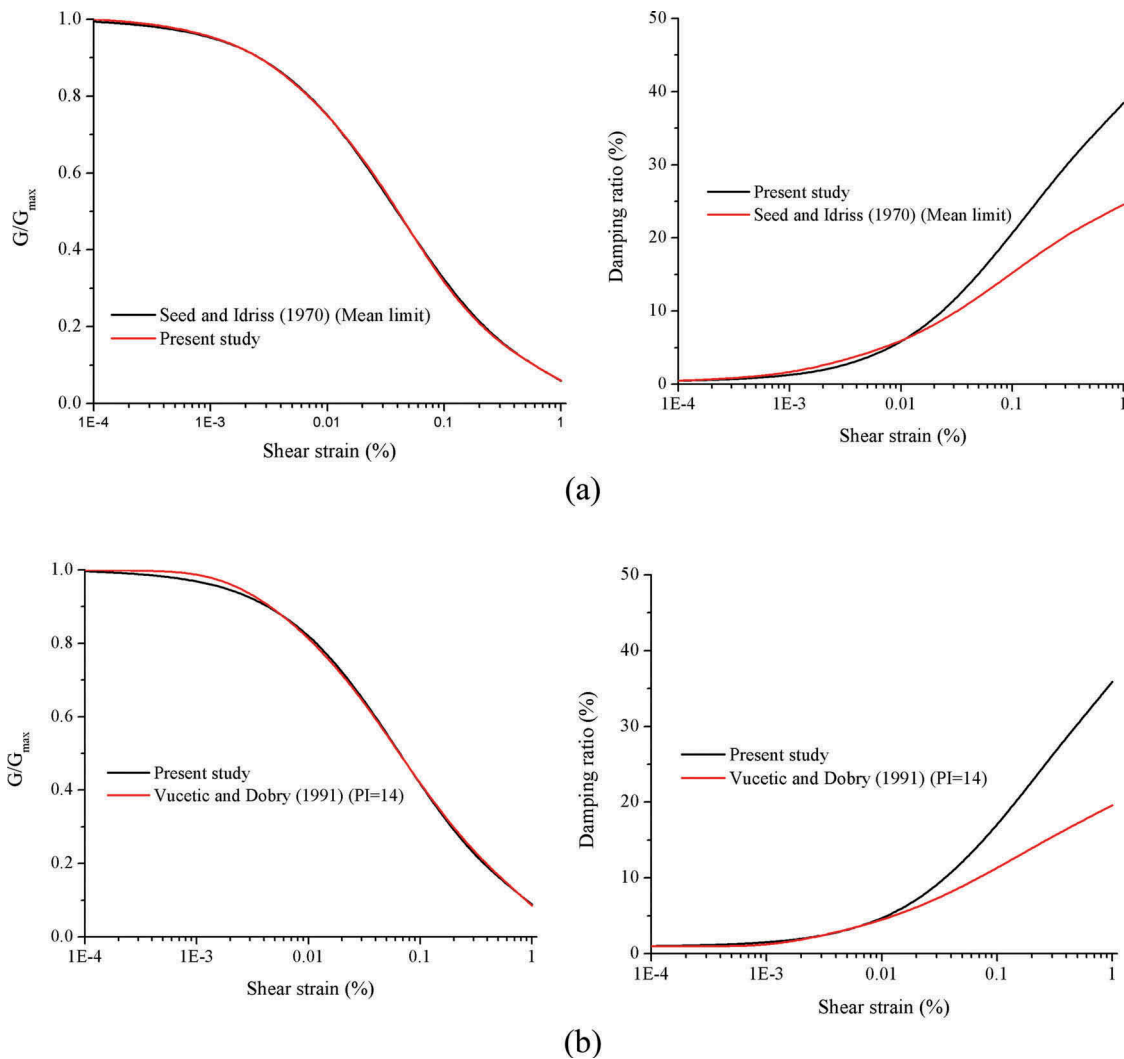


Figure 22. Comparison of G/G_{\max} and damping ratio (D) curves for (a) sand and clay with (b) $PI = 14$ (c) $PI = 24$ and (d) $PI = 42$.

frequency itself (Spears 2016). To dampen the artificial high-frequency components in the non-linear analysis in the response spectrum, a small amount of small strain damping such as, Rayleigh damping (= 1% for sand and 1.5% for clay) has been introduced (Miura *et al.* 2001). The equivalent linear analysis also underestimates the amplification ratio in high-frequency region thus rendering it incapable of producing higher modes of soil column during the dynamic excitation as shown in Figure 25. In addition, the equivalent linear analysis overestimates the amplification of acceleration at the natural frequency of the site in comparison to the nonlinear analysis. This stems from the underestimation of damping ratio in all the soil layers due to the concept of ‘effective strain’ in the equivalent linear method. Kim *et al.* (2016) have also made the similar

observation. Based on these observations, it may be concluded that a full-time domain, nonlinear analysis produces results which are more accurate and realistic than the equivalent linear methods and hence must be preferred.

6. Impact of loading-unloading rules on the frequency content of the surface spectrum

In this study, the loading and unloading rules influence the spectral values of the surface spectrum for a site. This finding is justified in this study by developing two nonlinear codes, in which the first one follows the Extended Masing rules (Xiaojun and Zheneng 1993) and the next one follows the rules proposed by Pyke (1979). The subject of interest is the spectral values on the surface which is used for

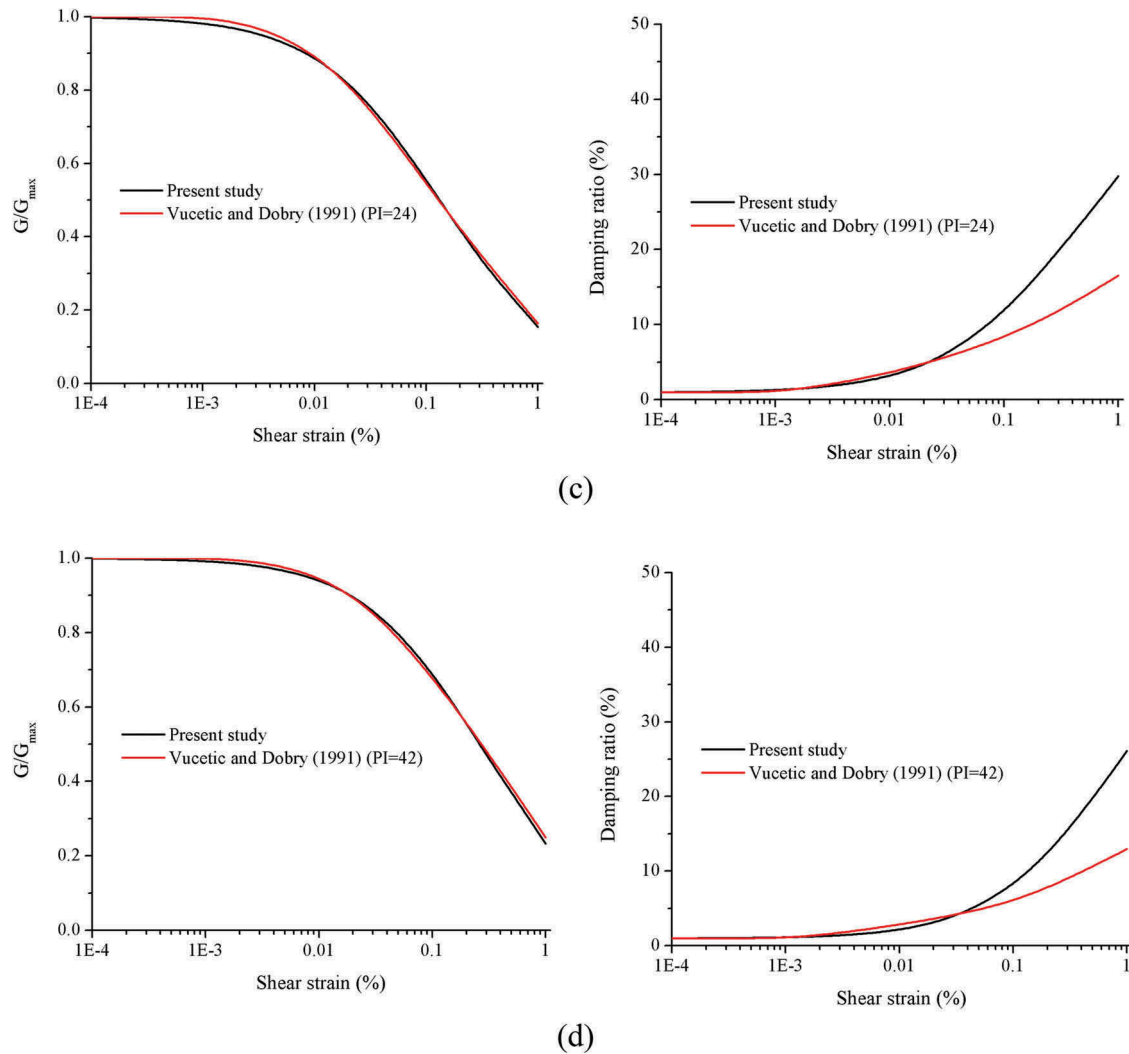


Figure 22. (Continued).

the design of superstructure, hence the comparison is made for the surface spectrum obtained from both the approaches for Site-1 and Site-2 as shown in Figure 26(a,b). From Figure 26(a,b), it is observed that the overall shape of the spectra obtained from both the approaches matches even at the higher modes of the soil column. But, the spectral value predicted at those frequencies decrease in the model based on Pyke's rules rather than for the model based on extended Masing rules. The spectral amplification at the natural frequency of the site obtained by the model based on extended Masing rules are 1.22 and 1.25 times more than those obtained by the model based on Pyke's rules. To accommodate site response analysis for nuclear (or stiff) facilities, the usage of these rules should be justified by some small-scale laboratory experiments.

7. Influence of low strain damping values on the generation of artificial high-frequency spectral values

In this study, it is found that the effect of low strain damping values on the non-linear models has a profound influence on the high-frequency spectral values as opposed by the findings by Hwang and Lee (1990). They stated that the low-strain damping ratio has only a minor influence on the site response analysis. This conclusion holds true in those cases in which the structural time period lies at 0.1 sec and above in which the spectral values do not change significantly. But in case of nuclear buildings (i.e. containment structure) and safety-related structure in which the time period is generally less than the ordinary buildings, the spectral values changes significantly with the changes in the low strain damping values.

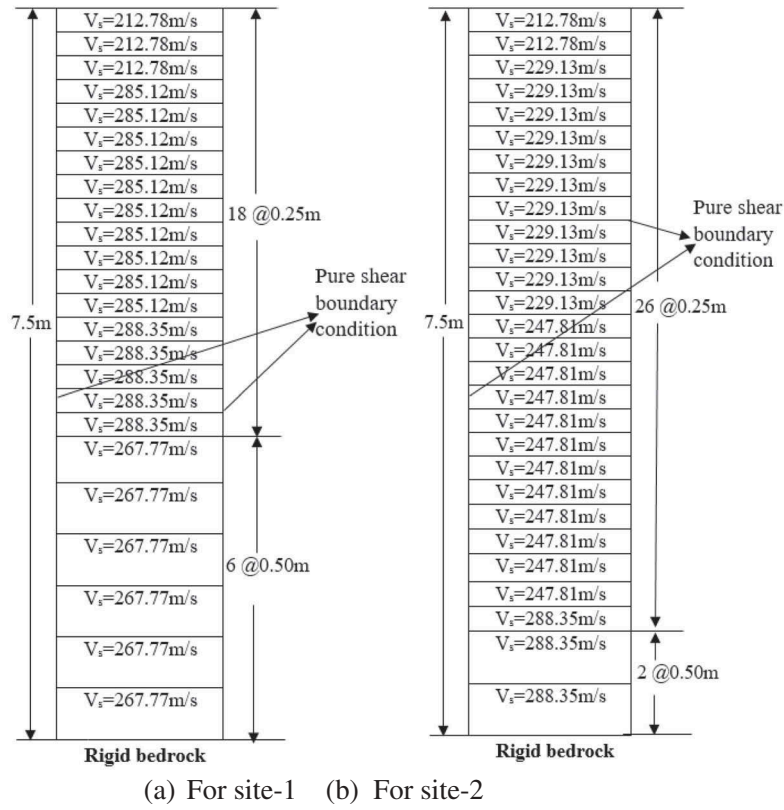


Figure 23. Discretisation of soil columns for (a) site-1 and (b) site-2 in Mumbai city.

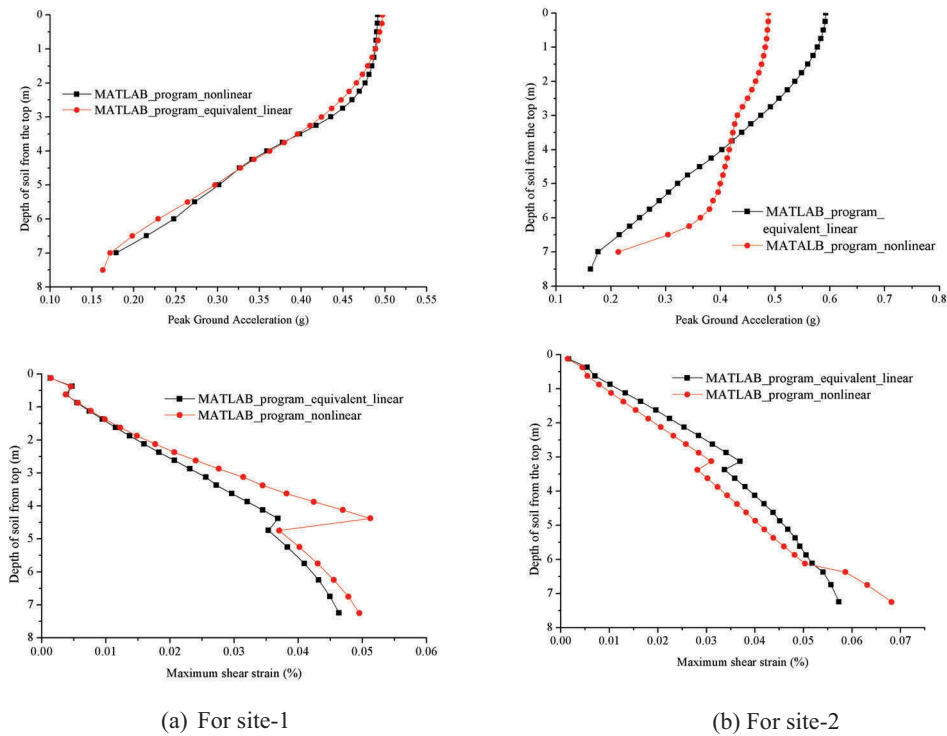


Figure 24. PGA and maximum shear strain at (a) site-1 and (b) site-2 for the selected ground motion.

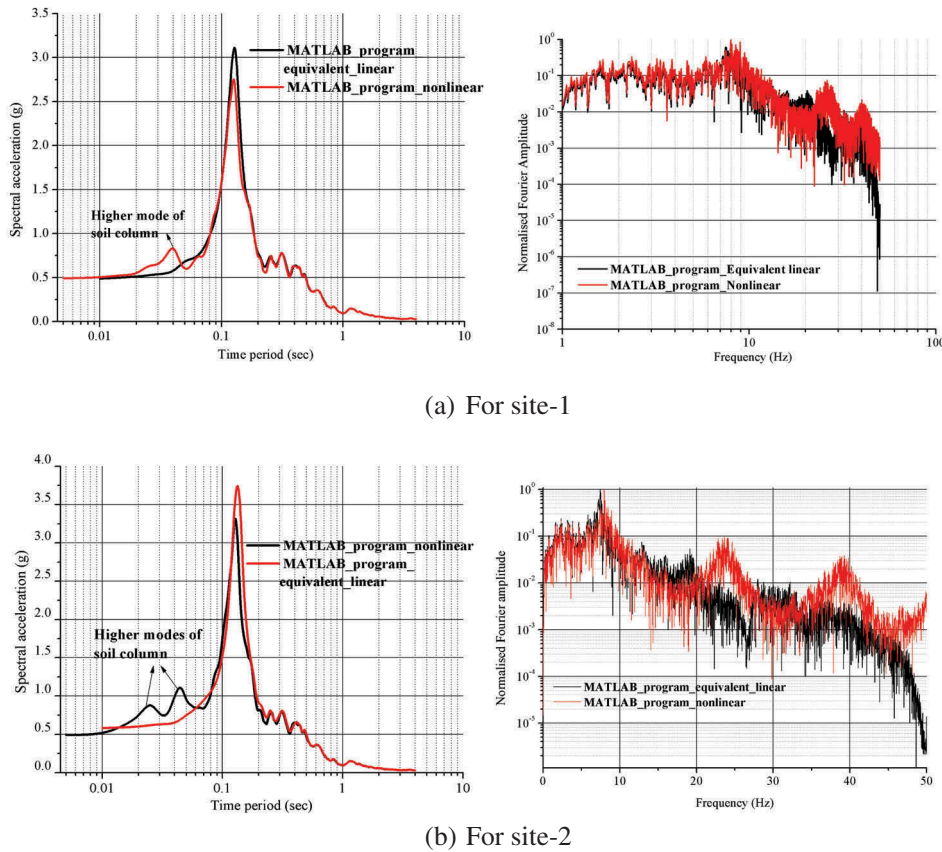


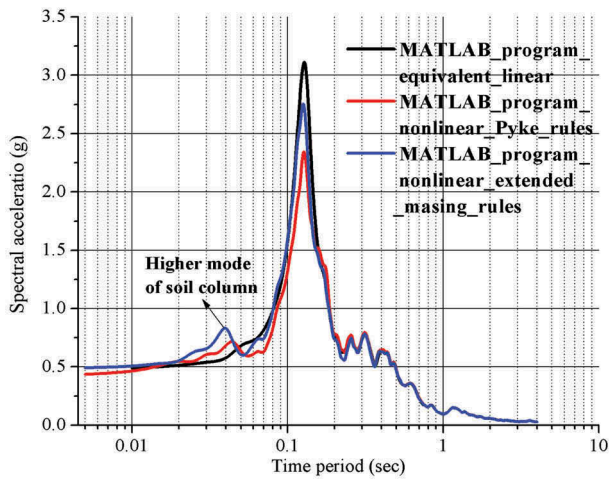
Figure 25. Response and Fourier spectrum at the surface of (a) Site-1 and (b) site-2 in Mumbai by equivalent and nonlinear analyses.

In this study, the effects of three sets of low strain damping values (0% for sand and clay, 0.1% and 0.15% for sand and clay, 1.0% and 1.5% for sand and clay) have been studied for Site-1 and Site-2 and are shown in Figure 27(a,b). It is seen from these figures that as the small strain damping values decrease, there is a gradual increase in the generation of artificial and real high-frequency components in the spectral values at both the sites. Thus, the PGA values also tend to be higher which can be seen from the following figures. To have a realistic estimate of the spectral values for the higher frequencies, it is proposed that a small strain damping of 1.0–1.5% is sufficient to remove the high-frequency noise (or the artificial high-frequency component) and keep the real higher frequencies intact (that is, the higher modes of the soil column). Hence, attention must be paid to the short-period region, since it is critical for calculation of seismic demands for nuclear (or stiff) facilities.

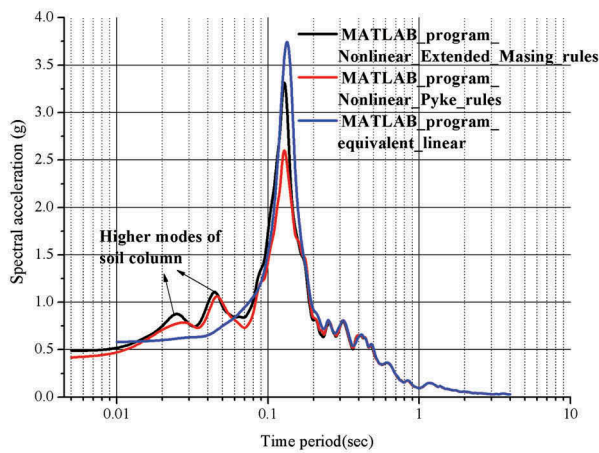
8. Conclusions

The equivalent linear and nonlinear ground response analyses at two typical Mumbai soil sites have been

presented for a spectral compatible motion of Imperial Valley Earthquake. The Imperial Valley Earthquake motion is selected based on its frequency contents and the original motion is arithmetically scaled to a PGA of 0.16 g for the present ground response analyses. It is observed that the local soil characteristics at the two sites have a profound influence on the ground responses. The natural frequency of the soil at Site-1 is 9.08 Hz. The natural frequency of soil at Site-2 is 8.12 Hz. The ground response by equivalent linear method shows amplification factors of 2.95 for Site-1 and 3.55 for Site-2. From the nonlinear analysis, the amplification factors for Site-1 and Site-2 are 2.88 and 2.84, respectively. The PGA values at the surface of Site-1 and Site-2 are 0.48 g and 0.478 g obtained from nonlinear analysis are in close agreement with the spectral acceleration values of 0.478 g and 0.497 g corresponding to the natural frequency of the two sites (9.08 Hz and 8.12 Hz) from the response spectra of Imperial Valley Earthquake. Based on the present results, it is recommended that the nonlinear analysis is preferred over the equivalent linear site response analysis as the PGA obtained at the surface is in line with the



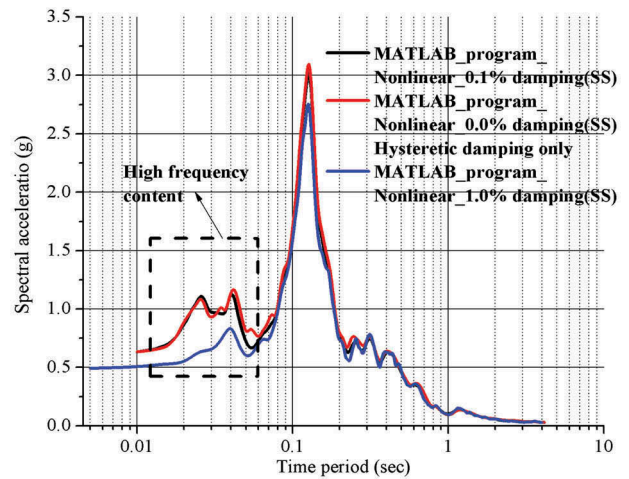
(a) For site-1



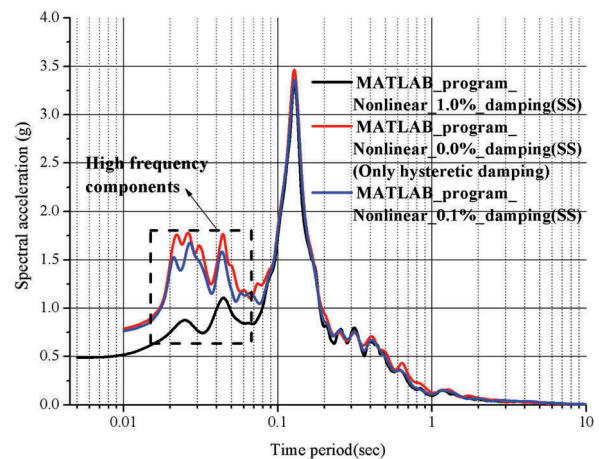
(b) For site-2

Figure 26. Comparison of surface spectrum obtained from extended Masing rules and Pyke rules in nonlinear analysis.

predicted values obtained from the response spectrum of Imperial Valley Earthquake (1979) which is compatible with the spectrum in the Indian building code, corresponding to the natural frequencies of the sites. The response spectra of the two sites, one on sand and another one on clay, may be readily used by engineers for the seismic analyses and design of superstructures in the city of Mumbai but with due caution regarding the loading-unloading rules used in the nonlinear analysis as well as the value of the small strain damping to be used in the nonlinear analysis. The recommended value of the small strain damping to be used in the nonlinear analysis of these sites is around 1–1.5%, which will predict the higher modes of the soil after suppressing the high-frequency noises with due accuracy.



(a) For site-1



(b) For site-2

Figure 27. Comparison of surface spectrum in the high-frequency region for different values of low strain damping.

Disclosure Statement

No potential conflict of interest was reported by the authors.

ORCID

Raj Banerjee  <http://orcid.org/0000-0002-0359-5738>

References

- Abel, J. and Shephard, M.S., 1979. An algorithm for multi-point constraints in finite element analysis. *International Journal for Numerical Methods in Engineering*, 14 (3), 464–467. doi:10.1002/()1097-0207
- Athanasopoulos, G.A., 1995. Empirical correlations $V_{so}-N_{SPT}$ for soils of Greece: a comparative study of reliability. In: *Proceedings of 7th international conference on soil dynamics*

- and earthquake engineering, Computation Mechanics Publications, Southampton, Boston, 19–25
- Chopra, A.K., 2001. *Dynamics of structures*. Englewood Cliffs: Prentice-Hall.
- Clough, R.W. and Penzien, J., 1993. *Dynamics of structures*. New York: McGraw-Hill.
- Coleman, J., Colleti, J., and Tessari, A., 2016. Large scale laminar box test plan. INL/EXT-16-39479, Structural Analysis, Idaho National Laboratory.
- Cook, R., Malkus, D.S., and Plesha, M.E., 1989. *Concepts and applications of finite element analysis*. New York: John Wiley and Sons, Inc.
- Dessai, A.G. and Bertrand, H., 1995. The panvel flexure along the Western Indian continental margin: an extensional fault structure related to deccan magmatism. *Tectonophysics*, 24 (1), 165–178. doi:10.1016/0040-1951(94)00077-M
- Hanumanthrao, C. and Ramana, G.V., 2008. Dynamic soil properties for microzonation of Delhi. India. *Journal of Earth System Science*, 117 (S2), 719–730. doi:10.1007/s12040-008-0066-2
- Hashash, Y.M.A., et al., 2012. DEEPSOIL 5.1 User Manual and Tutorial. doi:10.1094/PDIS-11-11-0999-PDN
- Hashash, Y.M.A. and Park, D., 2002. Viscous damping formulation and high frequency motion propagation in non-linear site response analysis. *Soil Dynamics and Earthquake Engineering*, 22, 611–624. doi:10.1016/S0267-7261(02)00042-8
- Hwang, H.H.M. and Lee, C.N., 1990. Parametric study of site response analysis. *Soil Dynamics and Earthquake Engineering*, 10 (6), 282–290. doi:10.1016/0267-7261(91)90045-2
- Imai, T. and Yoshimura, Y., 1970. Elastic wave velocity and soil properties in soft soil. *Tsuchito-Kiso*, 18 (1), 17–22. [in Japanese].
- IS:1893 (Part 1), 2002. *Indian standard criteria for earthquake resistant design of structures part1—general provisions and buildings (fifth revision)*. New Delhi: Bureau of Indian Standards.
- Itasca, 2005. *User's guide for FLAC version 5.0*. Nagpur, India: Itasca India Consulting.
- Jaiswal, K. and Sinha, R., 2007. Probabilistic seismic hazard estimation for peninsular India. *Bulletin of the Seismological Society of America*, 97 (1B), 318–330. doi:10.1785/0120050127
- Jinan, Z., 1987. Correlation between seismic wave velocity and the number of blow of SPT and depth. *Selected Papers from the Chinese Journal of Geotechnical Engineering ASCE*, 9, 92–100.
- Kaklamanos, J., et al., 2013. Critical parameters affecting bias and variability in site-response analyses using KiK-net downhole array data. *Bulletin of the Seismological Society of America*, 103 (3), 1733–1749. doi:10.1785/0120120166
- Kim, B., et al., 2016. Relative differences between nonlinear and equivalent-linear 1-D site response analyses. *Earthquake Spectra*, 32 (3), 1845–1865. doi:10.1193/051215EQS068M
- Kramer, S.L., 2005. *Geotechnical earthquake engineering*. Upper Saddle River: Prentice hall, Inc.
- Kramer, S.L. and Paulsen, S.B., 2004. *Practical use of geotechnical site response models. international workshop on uncertainties in nonlinear soil properties and their impact on modelling dynamic soil response*. UC Berkeley, USA: PEER.
- Kuhlemeyer, R.L. and Lysmer, J., 1973. Finite element method accuracy for wave propagation problems. *Journal of the Soil Mechanics and Foundations Division ASCE*, 99 (SM5), 421–427.
- Maheshwari, R.U., Boominathan, A., and Dodagoudar, G.R., 2010. Use of surface waves in statistical correlations of shear wave velocity and penetration resistance of Chennai soils. *Geotechnical and Geological Engineering*, 28, 119–137. doi:10.1007/s10706-009-9285-9
- Masing, G., 1926. Eigenspannungen und verfertigung beim Messing(C). *Proceedings of the 2nd International Congress on Applied Mechanics*, Zurich.
- Miura, K., Koyamada, K., and Iiba, M., 2001. Response spectrum method for evaluating nonlinear amplification of surface strata. *Journal of Structural and Construction Engineering Transaction of Architectural Institute of Japan*, 539, 57–62. doi:10.3130/aijs.66.57_1
- Nandy, D.R., 1995. Neotectonism and seismic hazards in India. *Indian Journal of Geosciences*, 67, 34–48.
- NEES, 2009. Ottawa F55 Sand. <https://nees.org/warehouse/specimen/project/122/experiment/4791>.
- Newmark, N.M., 1959. A method of computation for structural dynamics. *Journal of the Engineering Mechanics Division ASCE 85(EM3) Proc. Paper*, 2094, 67–94.
- Newmark, N.M., 1965. Effects of earthquakes on dams and embankments. *Geotechnique*, 15 (2), 139–159. doi:10.1680/geot.1965.15.2.139
- Ohsaki, Y. and Iwasaki, R., 1973. On dynamic shear moduli and Poisson's ratio of soil deposits. *Soils Found*, 13 (4), 61–73. doi:10.3208/sandf1972.13.4_61
- Pyke, R., 1979. Nonlinear soil models for irregular cyclic loadings. *Journal of Geotechnical Engineering Division, ASCE*, 105, 715–726.
- Rayleigh, J.W.S. and Lindsay, R.B., 1945. *The theory of sound*. New York: Dover Publications.
- Schnabel, P.B., Lysmer, J., and Seed, H.B., 1972. SHAKE—A computer program for earthquake response analysis of horizontally layered sites. EERC report Earthquake engineering.
- Seed, H.B. and Idriss, I.M., 1970. *Soil moduli and damping factors for dynamic response analysis*. EERC 70-10. Berkeley: University of California.
- Silva, W.J., et al., 2000. *Reassessment of site coefficient and near-fault factors for building code provisions*. El Cerrito, CA: Pacific engineering and analysis.
- Spears, B., 2016. NLSSI high frequency response study. INL/MIS-16-39106, Structural Analysis, Idaho National Laboratory.
- Spears, B. and Coleman, J., 2015. *Calibrating nonlinear soil material properties for seismic analysis using soil material properties intended for linear analysis*. SMIRT 23. Manchester, UK: IASMiRT.
- Stewart, J.P., et al., 2008. *Benchmarking of nonlinear geotechnical ground response analysis procedures*. Berkeley: Pacific Earthquake Engineering Research Center.
- Sykora, D.E. and Stokoe, K.H., 1983. Correlations of in-situ measurements in sands of shear wave velocity. *Soil Dynamics and Earthquake Engineering*, 20 (1), 125–136.

- Thevanayagam, S., Shenthan, T., and Kanagalingam, T., 2003. Role of intergranular contacts on mechanisms causing liquefaction & slope failures in silty sands. University at Buffalo, State University of New York, Department of Civil, Structural, and Environmental Engineering.
- Vucetic, M., 1990. Normalized behavior of clay under irregular cyclic loading. *Canadian Geotechnical Journal*, 27, 29–46. doi:10.1139/t90-004
- Vucetic, M. and Dobry, R., 1991. Effect of soil plasticity on cyclic response. *International Journal of Geotechnical Engineering*, 117 (1), 87–107. doi:10.1061/(ASCE)0733-9410(1991)117:1(89)
- Xiaojun, L. and Zheneng, L., 1993. Dynamic skeleton curve of soil stress strain relation under irregular cyclic loading. *Earthquake Research in China*, 7 (4), 469–477.
- Zalachoris, G. and Rathje, E., 2015. Comparisons of one-dimensional site response analysis and borehole array observations: quantification of bias and variability. *6th International Conference on Earthquake Geotechnical Engineering*, Christchurch, NZ.
- Zienkiewicz, O.C., et al., 1990. Static and dynamic behaviour of soils: a rational approach to quantitative solutions: i. fully saturated problems. *Proceedings of the Royal Society of London*, A429, 285–309.